



Introduction to Particle Detectors

with Particle Physics at the
Large Hadron Collider at CERN

Dr Clara Nellist

@ParticleClara

(she/her)

8th October 2024

CERN-Solvay Student Camp

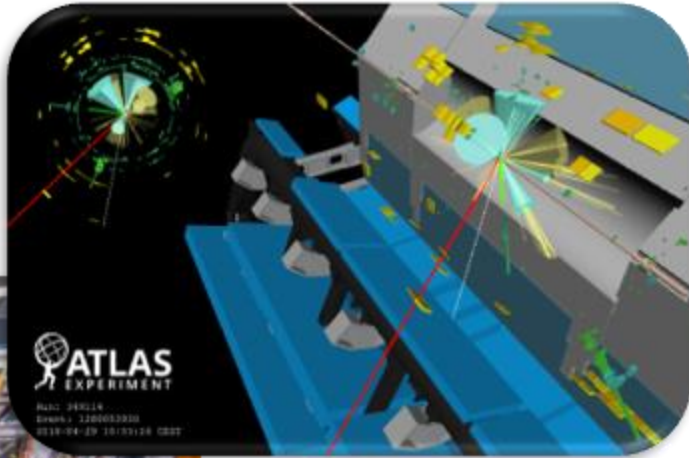
Nik|hef



 UNIVERSITEIT
VAN AMSTERDAM

Introduction to me

Particle physicist working on the ATLAS experiment



PhD in particle physics working on the ATLAS Experiment at CERN

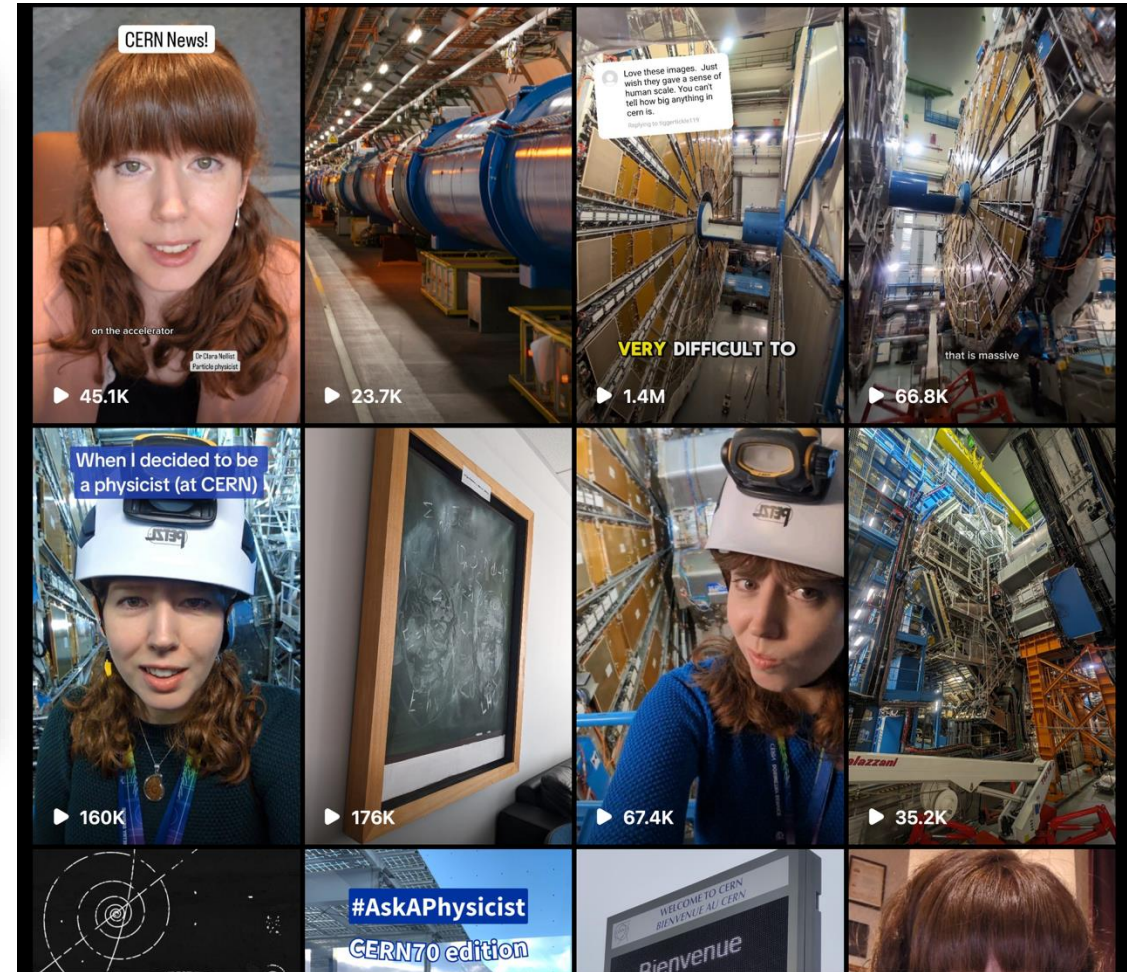
Research on 3D silicon pixel detectors for the Insertable B-Layer upgrade of ATLAS



Science Communicator



@ParticleClara everywhere



Voyage into the world of atoms

<https://videos.cern.ch/record/2307613>



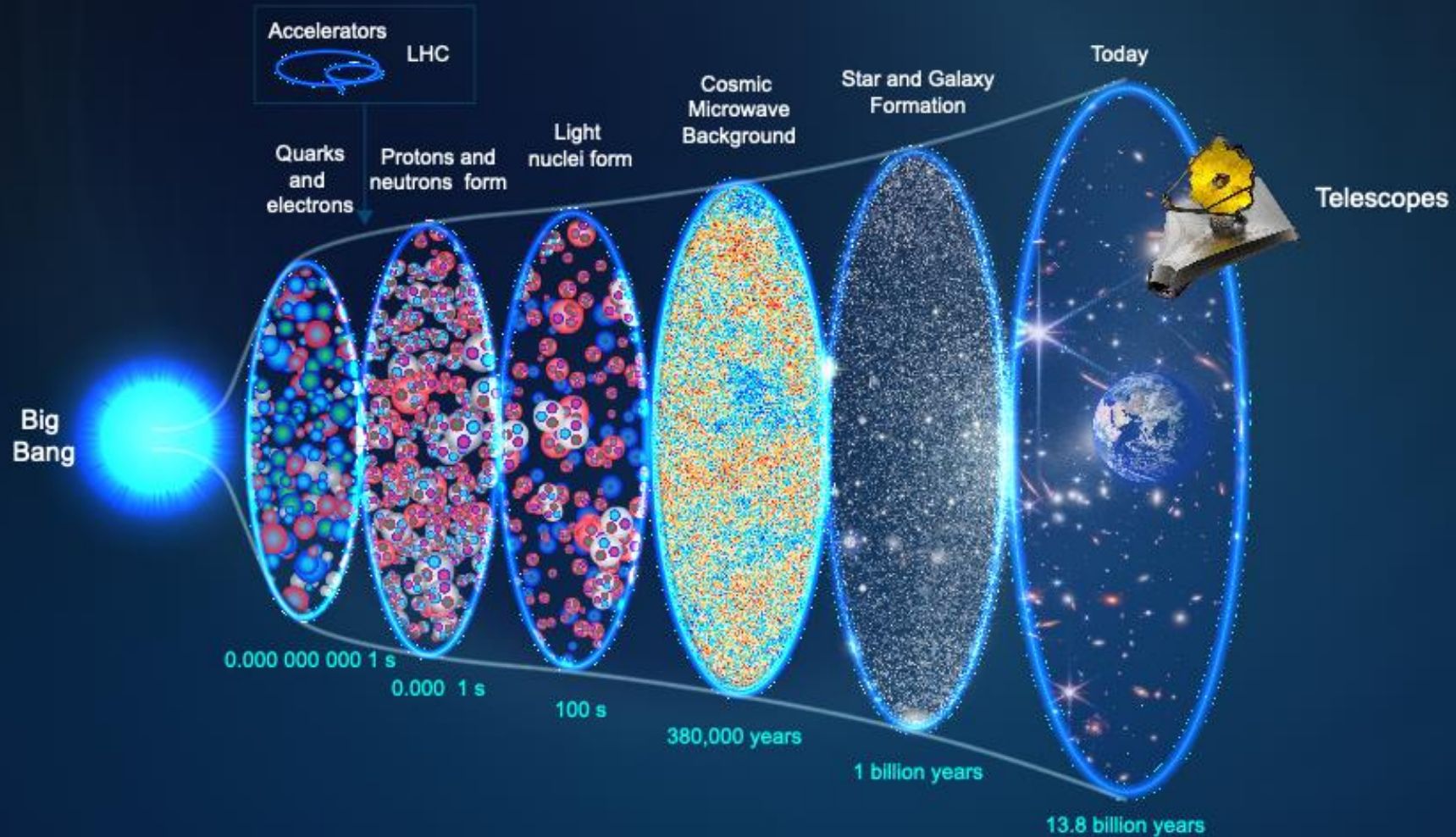
CERN



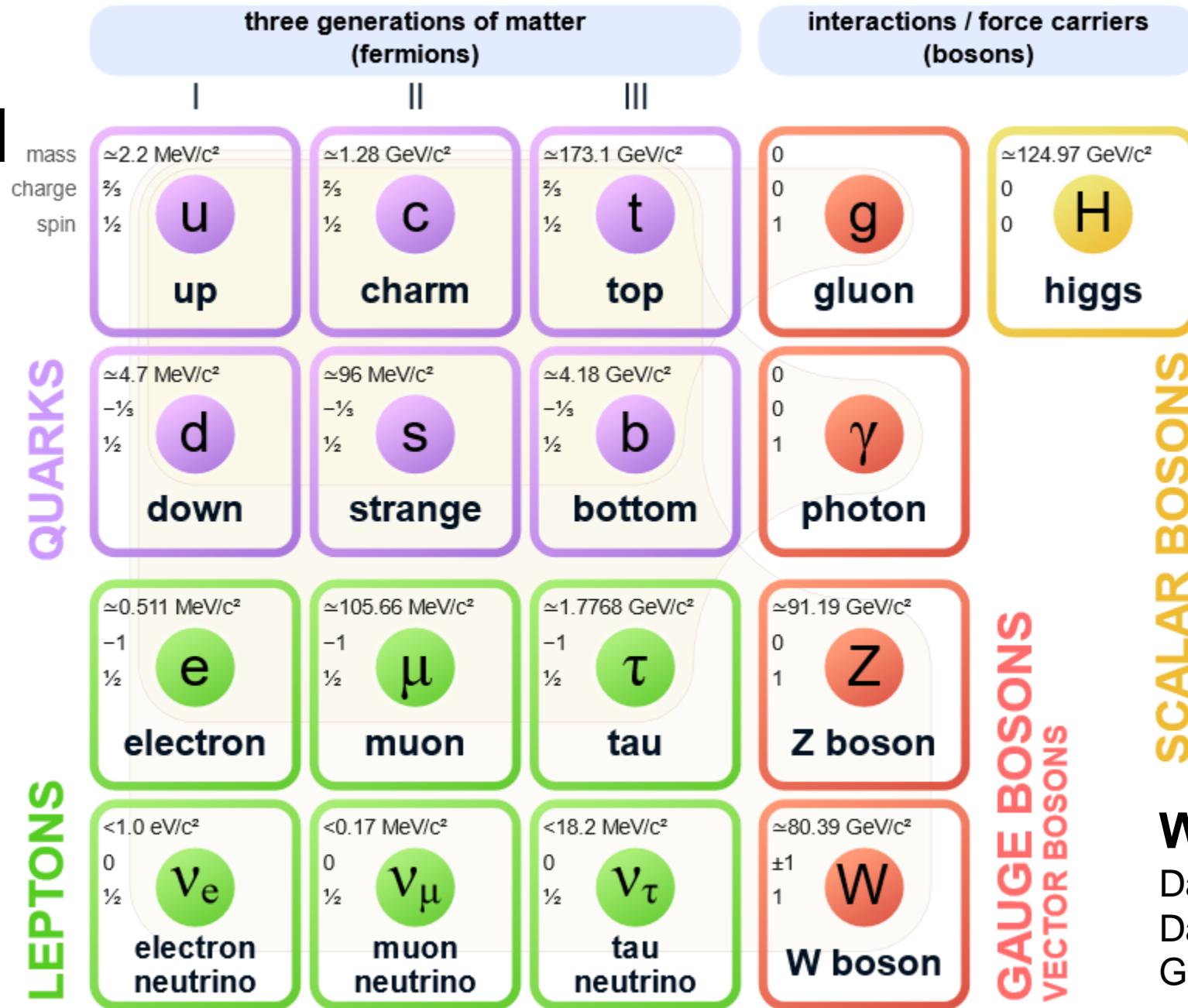
$$\begin{aligned}
& -\frac{1}{2}\partial_\nu g_\mu^a \partial_\nu g_\mu^a - g_s f^{abc} \partial_\mu g_\nu^b g_\mu^c g_\nu^c - \frac{1}{4}g_s^2 f^{abc} f^{ade} g_\mu^b g_\nu^c g_\mu^d g_\nu^e + \\
& \frac{1}{2}i g_s^2 (\bar{q}_i^\sigma \gamma^\mu q_j^\sigma) g_\mu^a + \bar{G}^a \partial^2 G^a + g_s f^{abc} \partial_\mu \bar{G}^a G^b g_\mu^c - \partial_\nu W_\mu^+ \partial_\nu W_\mu^- - \\
2 \quad & M^2 W_\mu^+ W_\mu^- - \frac{1}{2} \partial_\nu Z_\mu^0 \partial_\nu Z_\mu^0 - \frac{1}{2c_w^2} M^2 Z_\mu^0 Z_\mu^0 - \frac{1}{2} \partial_\mu A_\nu \partial_\mu A_\nu - \frac{1}{2} \partial_\mu H \partial_\mu H - \\
& \frac{1}{2} m_h^2 H^2 - \partial_\mu \phi^+ \partial_\mu \phi^- - M^2 \phi^+ \phi^- - \frac{1}{2} \partial_\mu \phi^0 \partial_\mu \phi^0 - \frac{1}{2c_w^2} M \phi^0 \phi^0 - \beta_h \left[\frac{2M^2}{g^2} + \right. \\
& \left. \frac{2M}{g} H + \frac{1}{2} (H^2 + \phi^0 \phi^0 + 2\phi^+ \phi^-) \right] + \frac{2M^4}{g^2} \alpha_h - igc_w [\partial_\nu Z_\mu^0 (W_\mu^+ W_\nu^- - \\
& W_\nu^+ W_\mu^-) - Z_\nu^0 (W_\mu^+ \partial_\nu W_\mu^- - W_\mu^- \partial_\nu W_\mu^+) + Z_\mu^0 (W_\nu^+ \partial_\nu W_\mu^- - \\
& W_\nu^- \partial_\nu W_\mu^+)] - ig s_w [\partial_\nu A_\mu (W_\mu^+ W_\nu^- - W_\nu^+ W_\mu^-) - A_\nu (W_\mu^+ \partial_\nu W_\mu^- - \\
& W_\mu^- \partial_\nu W_\mu^+) + A_\mu (W_\nu^+ \partial_\nu W_\mu^- - W_\nu^- \partial_\nu W_\mu^+)] - \frac{1}{2} g^2 W_\mu^+ W_\mu^- W_\nu^+ W_\nu^- + \\
& \frac{1}{2} g^2 W_\mu^+ W_\nu^- W_\mu^- W_\nu^+ + g^2 c_w^2 (Z_\mu^0 W_\mu^+ Z_\nu^0 W_\nu^- - Z_\mu^0 Z_\nu^0 W_\mu^+ W_\nu^-) + \\
& g^2 s_w^2 (A_\mu W_\mu^+ A_\nu W_\nu^- - A_\mu A_\nu W_\mu^+ W_\nu^-) + g^2 s_w c_w [A_\mu Z_\nu^0 (W_\mu^+ W_\nu^- - \\
& W_\nu^+ W_\mu^-) - 2A_\mu Z_\mu^0 W_\nu^+ W_\nu^-] - g\alpha [H^3 + H\phi^0 \phi^0 + 2H\phi^+ \phi^-] - \\
& \frac{1}{8} g^2 \alpha_h [H^4 + (\phi^0)^4 + 4(\phi^+ \phi^-)^2 + 4(\phi^0)^2 \phi^+ \phi^- + 4H^2 \phi^+ \phi^- + 2(\phi^0)^2 H^2] - \\
& g M W_\mu^+ W_\mu^- H - \frac{1}{2} g \frac{M}{c_w^2} Z_\mu^0 Z_\mu^0 H - \frac{1}{2} ig [W_\mu^+ (\phi^0 \partial_\mu \phi^- - \phi^- \partial_\mu \phi^0) - \\
& W_\mu^- (\phi^0 \partial_\mu \phi^+ - \phi^+ \partial_\mu \phi^0)] + \frac{1}{2} g [W_\mu^+ (H \partial_\mu \phi^- - \phi^- \partial_\mu H) - W_\mu^- (H \partial_\mu \phi^+ - \\
& \phi^+ \partial_\mu H)] + \frac{1}{2} g \frac{1}{c_w} (Z_\mu^0 (H \partial_\mu \phi^0 - \phi^0 \partial_\mu H) - ig \frac{s_w^2}{c_w} M Z_\mu^0 (W_\mu^+ \phi^- - W_\mu^- \phi^+) + \\
& ig s_w M A_\mu (W_\mu^+ \phi^- - W_\mu^- \phi^+) - ig \frac{1-2c_w^2}{2c_w} Z_\mu^0 (\phi^+ \partial_\mu \phi^- - \phi^- \partial_\mu \phi^+) + \\
& ig s_w A_\mu (\phi^+ \partial_\mu \phi^- - \phi^- \partial_\mu \phi^+) - \frac{1}{4} g^2 W_\mu^+ W_\mu^- [H^2 + (\phi^0)^2 + 2\phi^+ \phi^-] - \\
& \frac{1}{4} g^2 \frac{1}{c_w^2} Z_\mu^0 Z_\mu^0 [H^2 + (\phi^0)^2 + 2(2s_w^2 - 1)^2 \phi^+ \phi^-] - \frac{1}{2} g^2 \frac{s_w^2}{c_w} Z_\mu^0 \phi^0 (W_\mu^+ \phi^- + \\
& W_\mu^- \phi^+) - \frac{1}{2} ig^2 \frac{s_w^2}{c_w} Z_\mu^0 H (W_\mu^+ \phi^- - W_\mu^- \phi^+) + \frac{1}{2} g^2 s_w A_\mu \phi^0 (W_\mu^+ \phi^- + \\
& W_\mu^- \phi^+) + \frac{1}{2} ig^2 s_w A_\mu H (W_\mu^+ \phi^- - W_\mu^- \phi^+) - g^2 \frac{s_w}{c_w} (2c_w^2 - 1) Z_\mu^0 A_\mu \phi^+ \phi^- - \\
& g^1 s_w^2 A_\mu A_\mu \phi^+ \phi^- - \bar{e}^\lambda (\gamma \partial + m_e^\lambda) e^\lambda - \bar{\nu}^\lambda \gamma \partial \nu^\lambda - \bar{u}_j^\lambda (\gamma \partial + m_u^\lambda) u_j^\lambda - \\
3 \quad & \bar{d}_j^\lambda (\gamma \partial + m_d^\lambda) d_j^\lambda + ig s_w A_\mu [-(\bar{e}^\lambda \gamma^\mu e^\lambda) + \frac{2}{3} (\bar{u}_j^\lambda \gamma^\mu u_j^\lambda) - \frac{1}{3} (\bar{d}_j^\lambda \gamma^\mu d_j^\lambda)] + \\
& \frac{ig}{4c_w} Z_\mu^0 [(\bar{\nu}^\lambda \gamma^\mu (1 + \gamma^5) \nu^\lambda) + (\bar{e}^\lambda \gamma^\mu (4s_w^2 - 1 - \gamma^5) e^\lambda) + (\bar{u}_j^\lambda \gamma^\mu (\frac{4}{3}s_w^2 - \\
& 1 - \gamma^5) u_j^\lambda) + (\bar{d}_j^\lambda \gamma^\mu (1 - \frac{8}{3}s_w^2 - \gamma^5) d_j^\lambda)] + \frac{ig}{2\sqrt{2}} W_\mu^+ [(\bar{\nu}^\lambda \gamma^\mu (1 + \gamma^5) e^\lambda) + \\
& (\bar{u}_j^\lambda \gamma^\mu (1 + \gamma^5) C_{\lambda\kappa} d_j^\kappa)] + \frac{ig}{2\sqrt{2}} W_\mu^- [(\bar{e}^\lambda \gamma^\mu (1 + \gamma^5) \nu^\lambda) + (\bar{d}_j^\kappa C_{\lambda\kappa}^\dagger \gamma^\mu (1 + \\
& \gamma^5) u_j^\lambda)] + \frac{ig}{2\sqrt{2}} \frac{m_e^\lambda}{M} [-\phi^+ (\bar{\nu}^\lambda (1 - \gamma^5) e^\lambda) + \phi^- (\bar{e}^\lambda (1 + \gamma^5) \nu^\lambda)] - \\
4 \quad & \frac{g}{2} \frac{m_u^\lambda}{M} [H (\bar{e}^\lambda e^\lambda) + i\phi^0 (\bar{e}^\lambda \gamma^5 e^\lambda)] + \frac{ig}{2M\sqrt{2}} \phi^+ [-m_d^\kappa (\bar{u}_j^\lambda C_{\lambda\kappa} (1 - \gamma^5) d_j^\kappa) + \\
& m_u^\lambda (\bar{u}_j^\lambda C_{\lambda\kappa} (1 + \gamma^5) d_j^\kappa) + \frac{ig}{2M\sqrt{2}} \phi^- [m_d^\lambda (\bar{d}_j^\lambda C_{\lambda\kappa}^\dagger (1 + \gamma^5) u_j^\kappa) - m_u^\kappa (\bar{d}_j^\lambda C_{\lambda\kappa}^\dagger (1 - \\
& \gamma^5) u_j^\kappa) - \frac{g}{2} \frac{m_u^\lambda}{M} H (\bar{u}_j^\lambda u_j^\lambda) - \frac{g}{2} \frac{m_d^\lambda}{M} H (\bar{d}_j^\lambda d_j^\lambda) + \frac{ig}{2} \frac{m_u^\lambda}{M} \phi^0 (\bar{u}_j^\lambda \gamma^5 u_j^\lambda) - \\
& \frac{ig}{2} \frac{m_d^\lambda}{M} \phi^0 (\bar{d}_j^\lambda \gamma^5 d_j^\lambda)] + \bar{X}^+ (\partial^2 - M^2) X^+ + \bar{X}^- (\partial^2 - M^2) X^- + X^0 (\partial^2 - \\
5 \quad & \frac{M^2}{c_w^2}) X^0 + \bar{Y} \partial^2 Y + igc_w W_\mu^+ (\partial_\mu \bar{X}^0 X^- - \partial_\mu \bar{X}^+ X^0) + ig s_w W_\mu^+ (\partial_\mu \bar{Y} X^- - \\
& \partial_\mu \bar{X}^+ Y) + igc_w W_\mu^- (\partial_\mu \bar{X}^- X^0 - \partial_\mu \bar{X}^0 X^+) + ig s_w W_\mu^- (\partial_\mu \bar{X}^- Y - \\
& \partial_\mu \bar{Y} X^+) + igc_w Z_\mu^0 (\partial_\mu \bar{X}^+ X^+ - \partial_\mu \bar{X}^- X^-) + ig s_w A_\mu (\partial_\mu \bar{X}^+ X^+ - \\
& \partial_\mu \bar{X}^- X^-) - \frac{1}{2} g M [\bar{X}^+ X^+ H + \bar{X}^- X^- H + \frac{1}{c_w^2} \bar{X}^0 X^0 H] + \\
& \frac{1-2c_w^2}{2c_w} ig M [\bar{X}^+ X^0 \phi^+ - \bar{X}^- X^0 \phi^-] + \frac{1}{2c_w} ig M [\bar{X}^0 X^- \phi^+ - \bar{X}^0 X^+ \phi^-] + \\
& ig M s_w [\bar{X}^0 X^- \phi^+ - \bar{X}^0 X^+ \phi^-] + \frac{1}{2} ig M [\bar{X}^+ X^+ \phi^0 - \bar{X}^- X^- \phi^0]
\end{aligned}$$

But what are we looking for?

Studying nature's building blocks and the forces that govern them



The Standard Model



What's missing?

Dark matter
Dark energy
Gravity!

The Big Questions



Image: Jorge Cham / PhD Comics

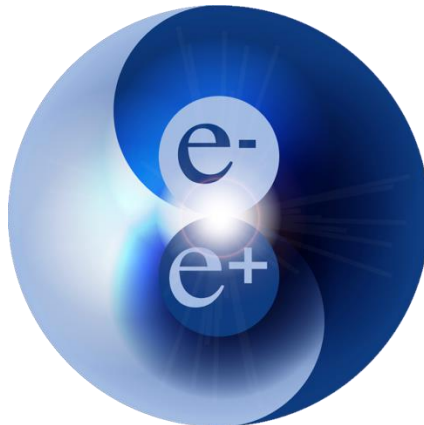
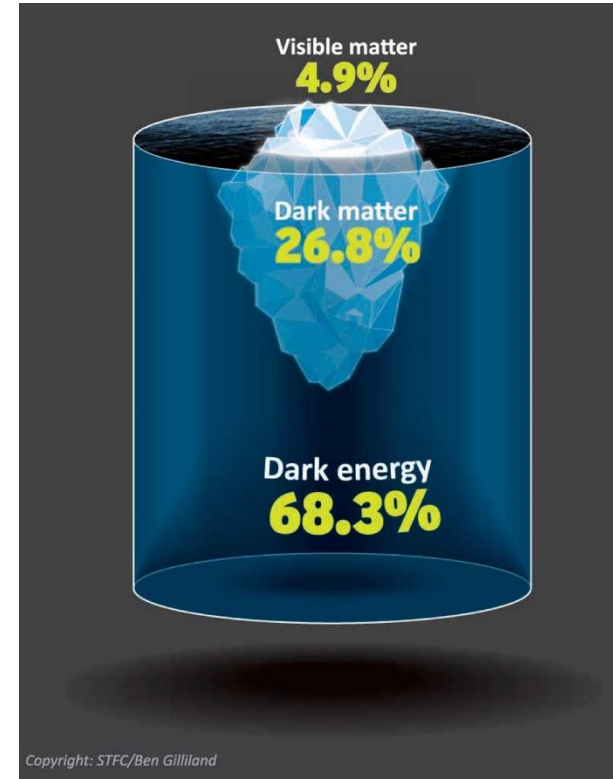


Illustration by Carolina Deluca / ATLAS © CERN

The search for the Higgs boson

But



WHY?

The search for the Higgs boson

Fun fact! If this happened very quickly, it might have caused gravitational echos that with bigger and better graviational waves detectors, maybe we can 'see' this

Aim: to understand the origin of the mass of elementary particles.



Image: Jorge Cham / PhD Comics

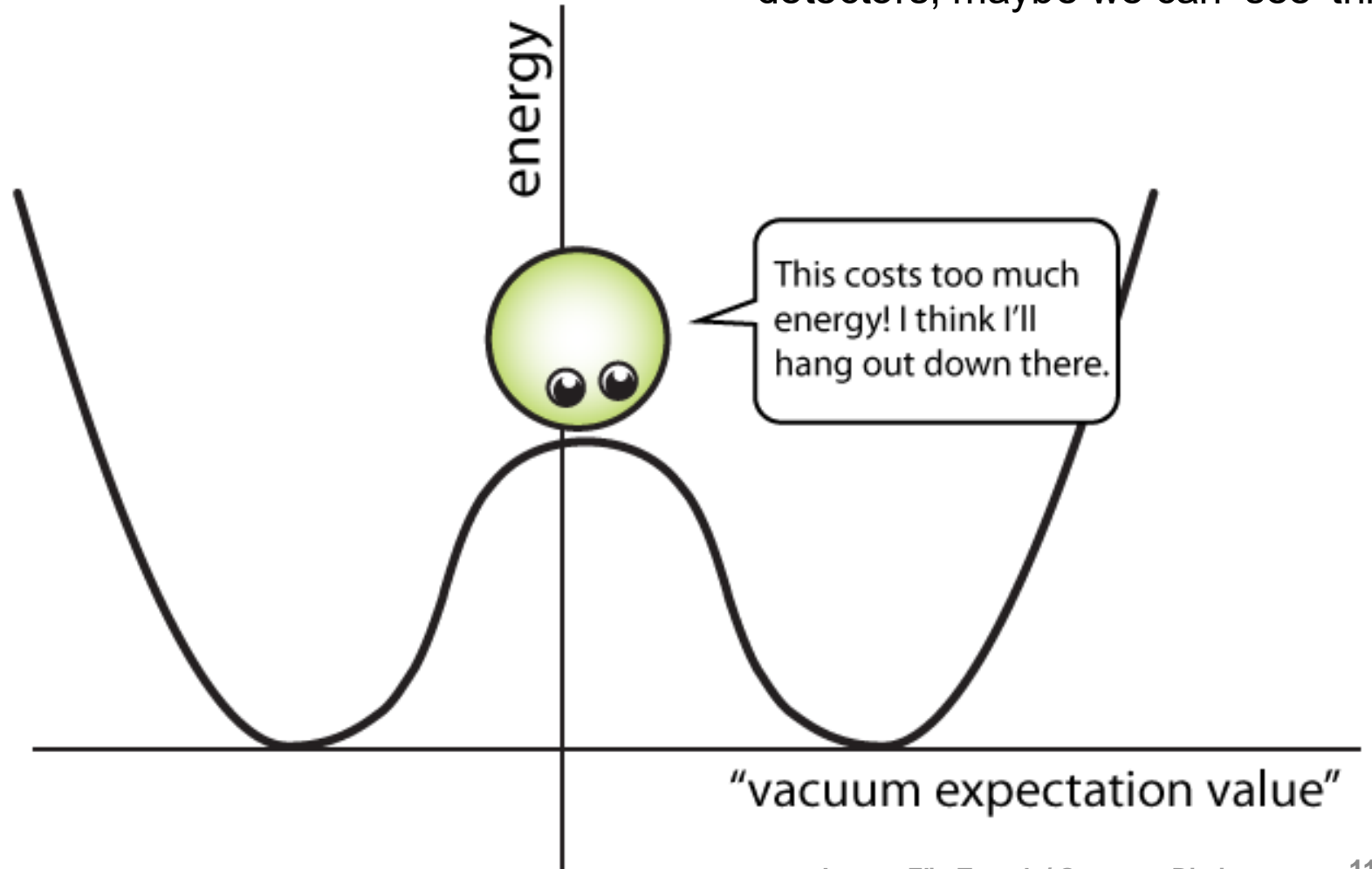


Image: Flip Tanedo/ Quantum Diaries

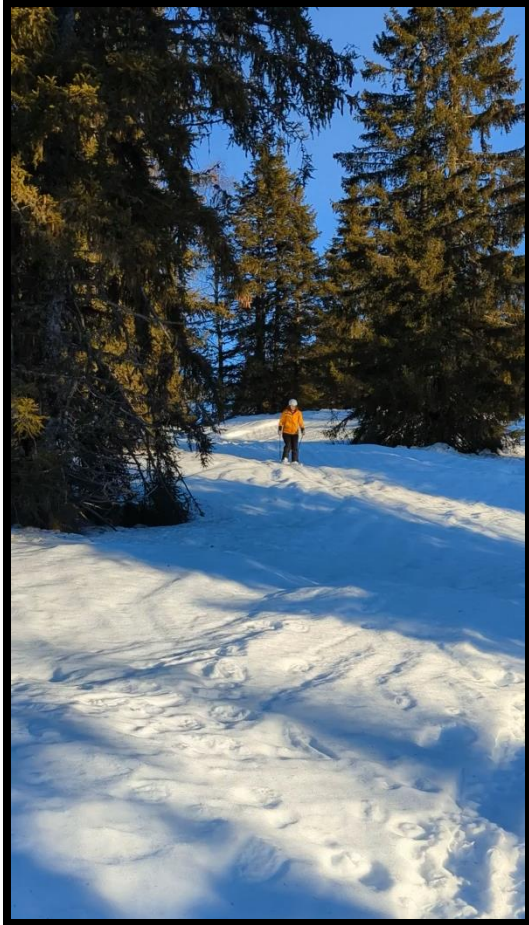
The Higgs boson



Image: Jorge Cham / PhD Comics

<https://youtu.be/71aIQCeCW6c>

Light particle



Heavy particle



The Higgs boson



The discovery of a new boson!

The Higgs boson – a major success of the first LHC run.



Physicists Find Elusive Particle Seen as Key to Universe

By DENNIS OVERBYE JULY 4, 2012



Scientists in Geneva on Wednesday applauded the discovery of a subatomic particle that looks like the Higgs boson. Pool photo by Denis Balibouse



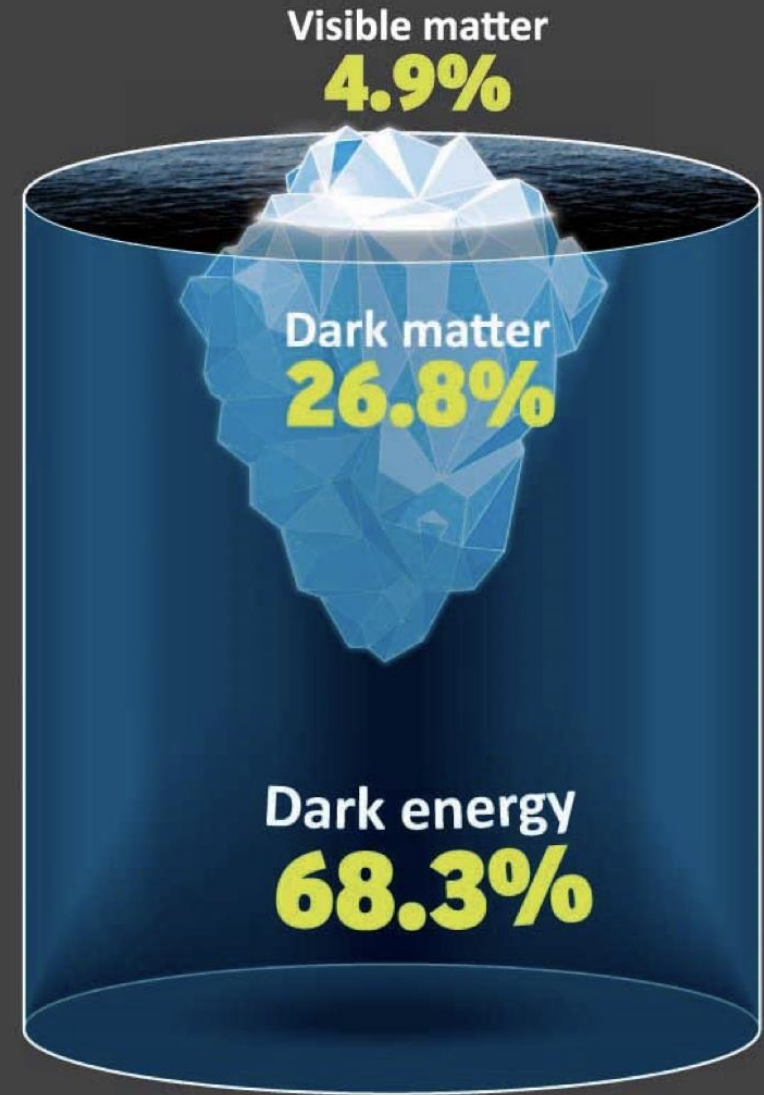
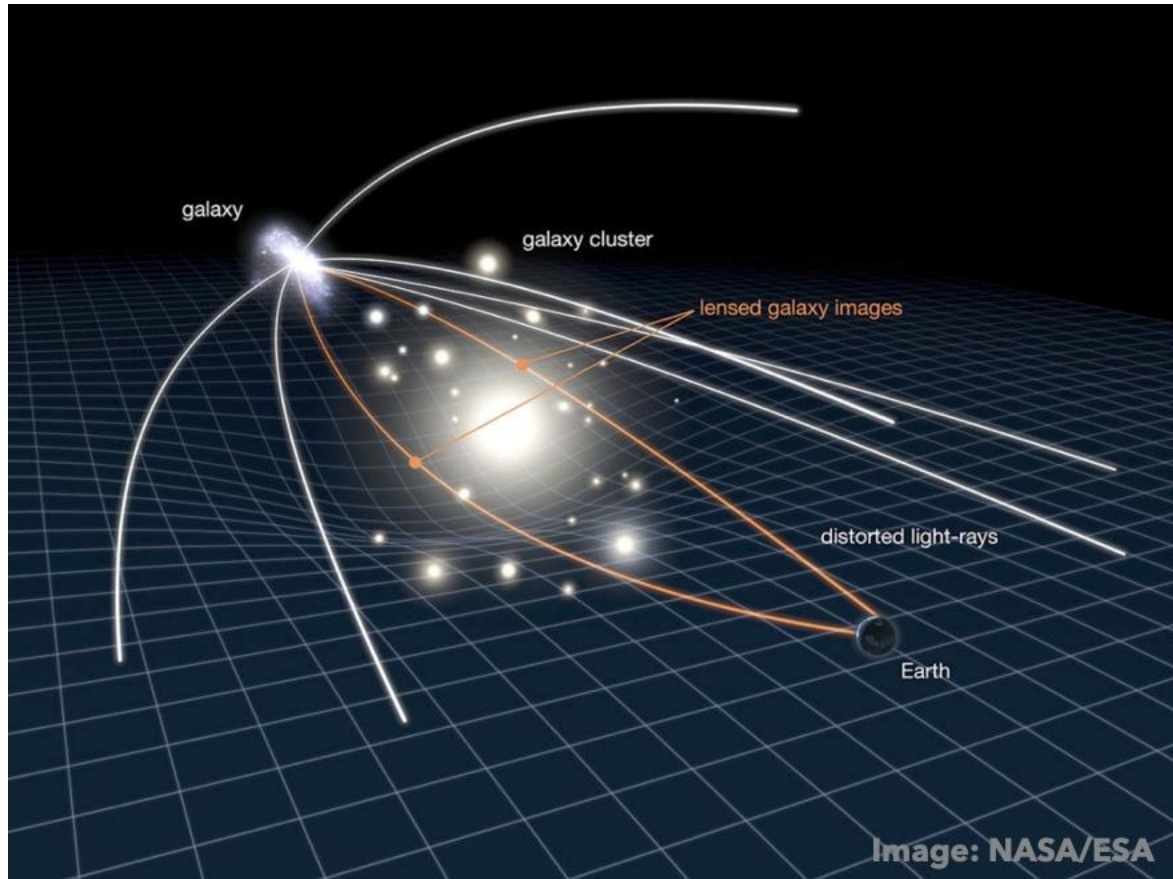


Combined results: the excess

Maximum excess observed at	$m_H = 126.5$ GeV
Local significance (including energy-scale systematics)	5.0σ
Probability of background up-fluctuation	3×10^{-7}
Expected from SM Higgs $m_H = 126.5$	4.6σ

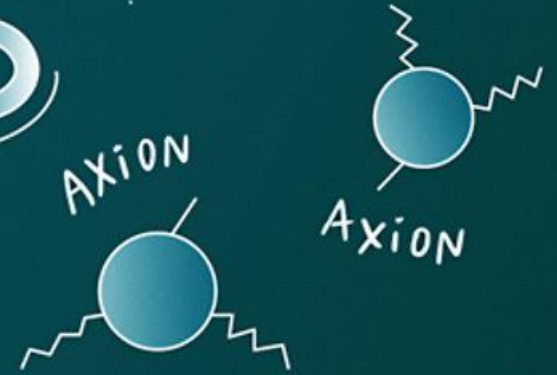
Global significance: $4.1-4.3 \sigma$ (for LEE over 110-600 or 110-150 GeV)

The search for new particles (dark matter?)

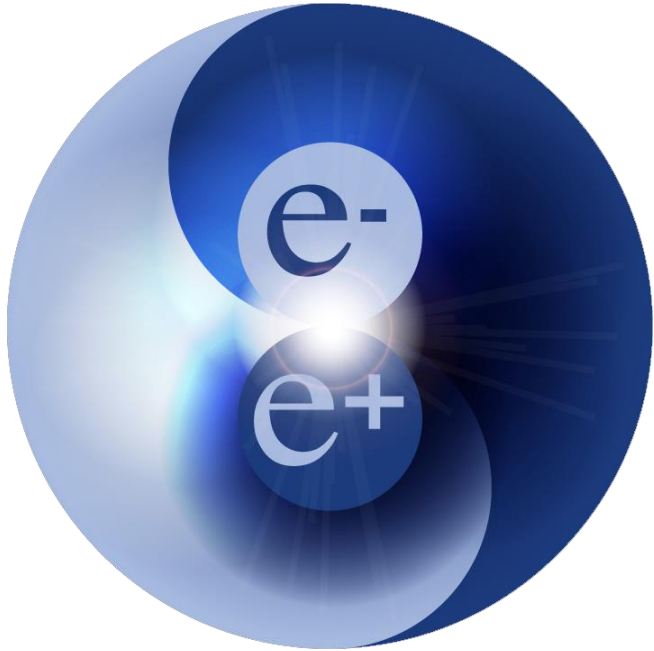


The search for

DARK MATTER



Matter-Antimatter asymmetry?



Note: originally detectors / scanners were people at CERN, often women:
<https://videos.cern.ch/record/2299808>

The Strength of Gravity?

- Is there a graviton?
- Are there extra dimensions that gravity is leaking into?
- What is the strength of gravity for antimatter?

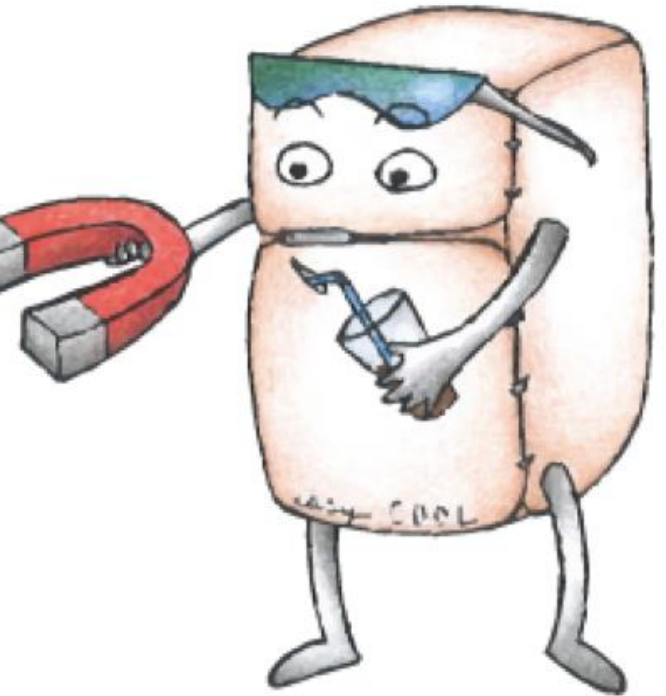


Illustration by Carolina Deluca / ATLAS © CERN

So, we keep searching

Searches

ATLAS Heavy Particle Searches* - 95% CL Upper Exclusion Limits

Status: March 2023

ATLAS Preliminary

$$\int \mathcal{L} dt = (3.6 - 139) \text{ fb}^{-1}$$

$$\sqrt{s} = 13 \text{ TeV}$$

Model	ℓ, γ	Jets [†]	E_T^{miss}	$\int \mathcal{L} dt [\text{fb}^{-1}]$	Limit	Reference	
Extra dimen.	ADD $G_{KK} + g/q$	$0 e, \mu, \tau, \gamma$	$1-4 j$	Yes	139	M_D 11.2 TeV $n=2$	2102.10874
	ADD non-resonant $\gamma\gamma$	2γ	-	-	36.7	M_S 8.6 TeV $n=3$ HLZ NLO	1707.04147
	ADD QBH	-	$2 j$	-	139	M_{th} 9.4 TeV $n=6$	1910.08447
	ADD BH multijet	-	$\geq 3 j$	-	3.6	M_{th} 9.55 TeV $n=6, M_D = 3 \text{ TeV, rot BH}$	1512.02586
	RS1 $G_{KK} \rightarrow \gamma\gamma$	2γ	-	-	139	$G_{KK} \text{ mass}$ 4.5 TeV $k/\overline{M}_{Pl} = 0.1$	2102.13405
	Bulk RS $G_{KK} \rightarrow WW/ZZ$	multi-channel	-	-	36.1	$G_{KK} \text{ mass}$ 2.3 TeV $k/\overline{M}_{Pl} = 1.0$	1808.02380
	Bulk RS $g_{KK} \rightarrow tt$	$1 e, \mu$	$\geq 1 b, \geq 1 J/2j$	Yes	36.1	$g_{KK} \text{ mass}$ 3.8 TeV $\Gamma/m = 15\%$	1804.10823
	2UED / RPP	$1 e, \mu$	$\geq 2 b, \geq 3 j$	Yes	36.1	KK mass 1.8 TeV Tier (1,1), $\mathcal{B}(A^{(1,1)} \rightarrow tt) = 1$	1803.09678
Gauge bosons	SSM $Z' \rightarrow \ell\ell$	$2 e, \mu$	-	-	139	$Z' \text{ mass}$ 5.1 TeV	1903.06248
	SSM $Z' \rightarrow \tau\tau$	2τ	-	-	36.1	$Z' \text{ mass}$ 2.42 TeV	1709.07242
	Leptophobic $Z' \rightarrow bb$	-	$2 b$	-	36.1	$Z' \text{ mass}$ 2.1 TeV	1805.09299
	Leptophobic $Z' \rightarrow tt$	$0 e, \mu$	$\geq 1 b, \geq 2 J$	Yes	139	$Z' \text{ mass}$ 4.1 TeV $\Gamma/m = 1.2\%$	2005.05138
	SSM $W' \rightarrow \ell\nu$	$1 e, \mu$	-	Yes	139	$W' \text{ mass}$ 6.0 TeV	1906.05609
	SSM $W' \rightarrow \tau\nu$	1τ	-	Yes	139	$W' \text{ mass}$ 5.0 TeV	ATLAS-CONF-2021-025
	SSM $W' \rightarrow tb$	-	$\geq 1 b, \geq 1 J$	-	139	$W' \text{ mass}$ 4.4 TeV	ATLAS-CONF-2021-043
	HVT $W' \rightarrow WZ$ model B	$0-2 e, \mu$	$2 j / 1 J$	Yes	139	$W' \text{ mass}$ 4.3 TeV $g_V = 3$	2004.14636
	HVT $W' \rightarrow WZ \rightarrow \ell\nu \ell'\ell'$ model C	$3 e, \mu$	$2 j$ (VBF)	Yes	139	$W' \text{ mass}$ 340 GeV $g_V c_H = 1, g_R = 0$	2207.03925
	HVT $Z' \rightarrow WW$ model B	$1 e, \mu$	$2 j / 1 J$	Yes	139	$Z' \text{ mass}$ 3.9 TeV $g_V = 3$	2004.14636
LRSM $W_R \rightarrow \mu N_R$	2μ	$1 J$	-	80	$W_R \text{ mass}$ 5.0 TeV $m(N_R) = 0.5 \text{ TeV, } g_L = g_R$	1904.12679	
CI	CI $qqqq$	-	$2 j$	-	37.0	Λ 21.8 TeV η_{LL}	1703.09127
	CI $\ell\ell qq$	$2 e, \mu$	-	-	139	Λ 35.8 TeV η_{LL}	2006.12946
	CI $eebs$	$2 e$	$1 b$	-	139	Λ 1.8 TeV $g_s = 1$	2105.13847
	CI $\mu\mu bs$	2μ	$1 b$	-	139	Λ 2.0 TeV $g_s = 1$	2105.13847
	CI $tttt$	$\geq 1 e, \mu$	$\geq 1 b, \geq 1 j$	Yes	36.1	Λ 2.57 TeV $ C_{4\ell} = 4\pi$	1811.02305
DM	Axial-vector med. (Dirac DM)	-	$2 j$	-	139	m_{med} 3.8 TeV $g_q = 0.25, g_\ell = 1, m(\chi) = 10 \text{ GeV}$	ATL-PHYS-PUB-2022-036
	Pseudo-scalar med. (Dirac DM)	$0 e, \mu, \tau, \gamma$	$1-4 j$	Yes	139	m_{med} 376 GeV $g_q = 1, g_\ell = 1, m(\chi) = 1 \text{ GeV}$	2102.10874
	Vector med. Z' -2HDM (Dirac DM)	$0 e, \mu$	$2 b$	Yes	139	$m_{Z'}$ 3.0 TeV $\tan\beta = 1, g_Z = 0.8, m(\chi) = 100 \text{ GeV}$	2108.13391
Pseudo-scalar med. 2HDM+a	multi-channel	-	-	139	m_a 800 GeV $\tan\beta = 1, g_\ell = 1, m(\chi) = 10 \text{ GeV}$	ATLAS-CONF-2021-036	
LQ	Scalar LQ 1 st gen	$2 e$	$\geq 2 j$	Yes	139	LQ mass 1.8 TeV $\beta = 1$	2006.05872
	Scalar LQ 2 nd gen	2μ	$\geq 2 j$	Yes	139	LQ mass 1.7 TeV $\beta = 1$	2006.05872
	Scalar LQ 3 rd gen	1τ	$2 b$	Yes	139	LQ ^u mass 1.49 TeV $\mathcal{B}(LQ_3^u \rightarrow b\tau) = 1$	2303.01294
	Scalar LQ 3 rd gen	$0 e, \mu$	$\geq 2 j, \geq 2 b$	Yes	139	LQ ^d mass 1.24 TeV $\mathcal{B}(LQ_3^d \rightarrow t\nu) = 1$	2004.14060
	Scalar LQ 3 rd gen	$\geq 2 e, \mu, \geq 1 \tau, \geq 1 j, \geq 1 b$	-	-	139	LQ ^s mass 1.43 TeV $\mathcal{B}(LQ_3^s \rightarrow t\tau) = 1$	2101.11582
	Scalar LQ 3 rd gen	$0 e, \mu, \geq 1 \tau, 0-2 j, 2 b$	Yes	139	LQ ^s mass 1.26 TeV $\mathcal{B}(LQ_3^s \rightarrow b\nu) = 1$	2101.12527	
	Vector LQ mix gen	multi-channel	$\geq 1 j, \geq 1 b$	Yes	139	LQ ^v mass 2.0 TeV $\mathcal{B}(\tilde{U}_1 \rightarrow t\mu) = 1, \text{Y-M coupl.}$	ATLAS-CONF-2022-052
	Vector LQ 3 rd gen	$2 e, \mu, \tau$	$\geq 1 b$	Yes	139	LQ ^v mass 1.96 TeV $\mathcal{B}(LQ_3^v \rightarrow b\tau) = 1, \text{Y-M coupl.}$	2303.01294
Vector-like fermions	VLQ $TT \rightarrow Zt + X$	$2e/2\mu \geq 3e, \mu$	$\geq 1 b, \geq 1 j$	-	139	T mass 1.46 TeV SU(2) doublet	2210.15413
	VLQ $BB \rightarrow Wt/Zb + X$	multi-channel	-	-	36.1	B mass 1.34 TeV SU(2) doublet	1808.02343
	VLQ $T_{5/3} T_{5/3} T_{5/3} \rightarrow Wt + X$	$2(SS) \geq 3 e, \mu$	$\geq 1 b, \geq 1 j$	Yes	36.1	$T_{5/3} \text{ mass}$ 1.64 TeV $\mathcal{B}(T_{5/3} \rightarrow Wt) = 1, c(T_{5/3} Wt) = 1$	1807.11883
	VLQ $T \rightarrow Ht/Zt$	$1 e, \mu$	$\geq 1 b, \geq 3 j$	Yes	139	T mass 1.8 TeV SU(2) singlet, $\kappa_T = 0.5$	ATLAS-CONF-2021-040
	VLQ $Y \rightarrow Wb$	$1 e, \mu$	$\geq 1 b, \geq 1 j$	Yes	36.1	Y mass 1.85 TeV $\mathcal{B}(Y \rightarrow Wb) = 1, c_R(Wb) = 1$	1812.07343
	VLQ $B \rightarrow Hb$	$0 e, \mu$	$\geq 2b, \geq 1j, \geq 1J$	-	139	B mass 2.0 TeV SU(2) doublet, $\kappa_B = 0.3$	ATLAS-CONF-2021-018
	VLL $\tau' \rightarrow Z\tau/H\tau$	multi-channel	$\geq 1 j$	Yes	139	$\tau' \text{ mass}$ 898 GeV SU(2) doublet	2303.05441
Exctd ferm.	Excited quark $q^* \rightarrow qg$	-	$2 j$	-	139	$q^* \text{ mass}$ 6.7 TeV only u^* and $d^*, \Lambda = m(q^*)$	1910.08447
	Excited quark $q^* \rightarrow q\gamma$	1γ	$1 j$	-	36.7	$q^* \text{ mass}$ 5.3 TeV only u^* and $d^*, \Lambda = m(q^*)$	1709.10440
	Excited quark $b^* \rightarrow bg$	-	$1 b, 1 j$	-	139	$b^* \text{ mass}$ 3.2 TeV	1910.08447
	Excited lepton τ^*	2τ	$\geq 2 j$	-	139	$\tau^* \text{ mass}$ 4.6 TeV $\Lambda = 4.6 \text{ TeV}$	2303.09444
Other	Type III Seesaw	$2, 3, 4 e, \mu$	$\geq 2 j$	Yes	139	$N^0 \text{ mass}$ 910 GeV	2202.02039
	LRSM Majorana ν	2μ	$2 j$	-	36.1	$N_R \text{ mass}$ 3.2 TeV	1809.11105
	Higgs triplet $H^{++} \rightarrow W^\pm W^\pm$	$2, 3, 4 e, \mu$ (SS)	various	Yes	139	$H^{++} \text{ mass}$ 350 GeV $m(W_R) = 4.1 \text{ TeV, } g_L = g_R$	2101.11961
	Higgs triplet $H^{++} \rightarrow \ell\ell$	$2, 3, 4 e, \mu$ (SS)	-	-	139	$H^{++} \text{ mass}$ 1.08 TeV DY production	2211.07505
	Multi-charged particles	-	-	-	139	multi-charged particle mass 1.59 TeV DY production, $ q = 5e$	ATLAS-CONF-2022-034
	Magnetic monopoles	-	-	-	34.4	monopole mass 2.37 TeV DY production, $ g = 1g_D, \text{spin } 1/2$	1905.10130

$\sqrt{s} = 13 \text{ TeV}$
partial data $\sqrt{s} = 13 \text{ TeV}$
full data

10⁻¹ 1 10 Mass scale [TeV]

*Only a selection of the available mass limits on new states or phenomena is shown.

† Small-radius (large-radius) jets are denoted by the letter j (J).

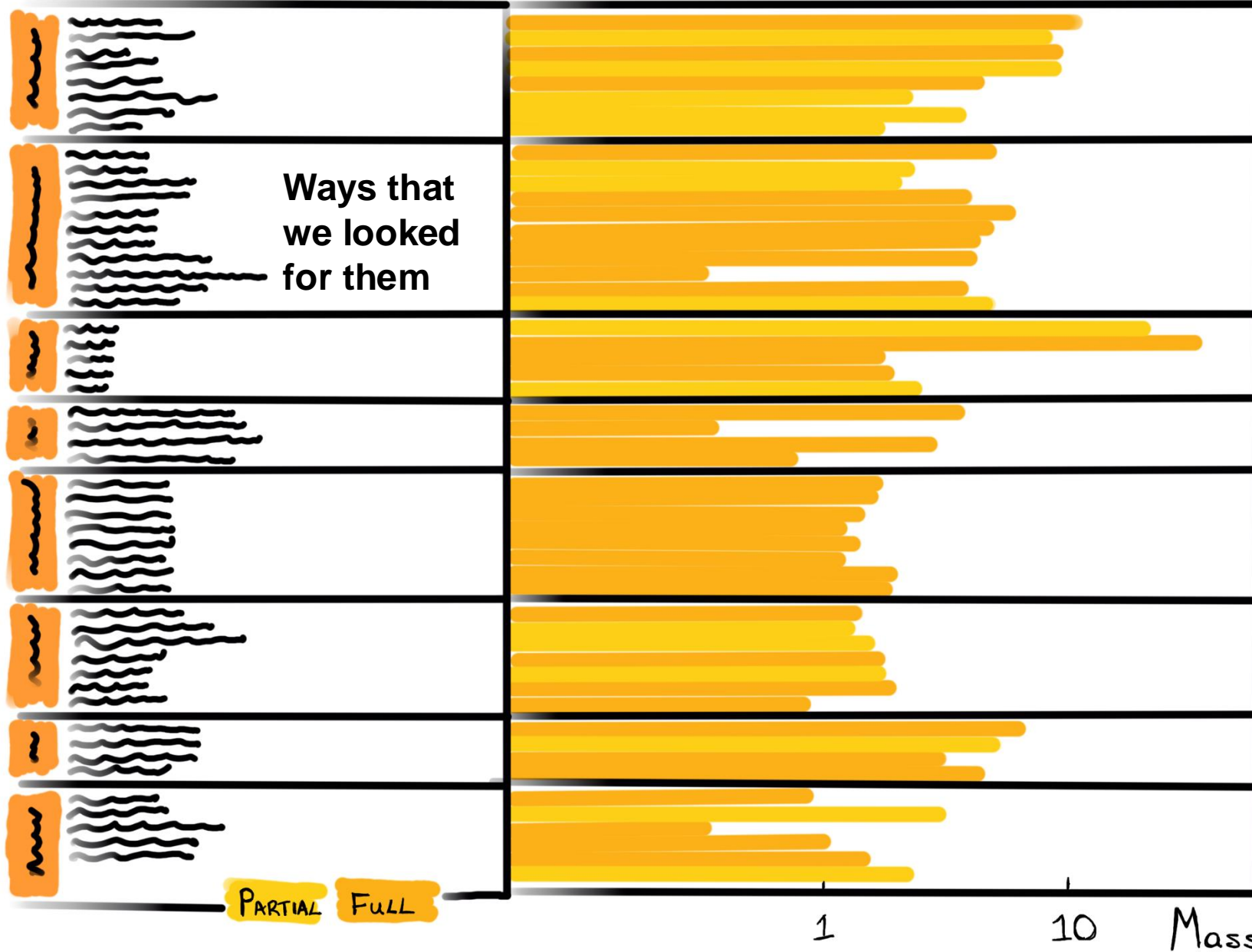
Searches

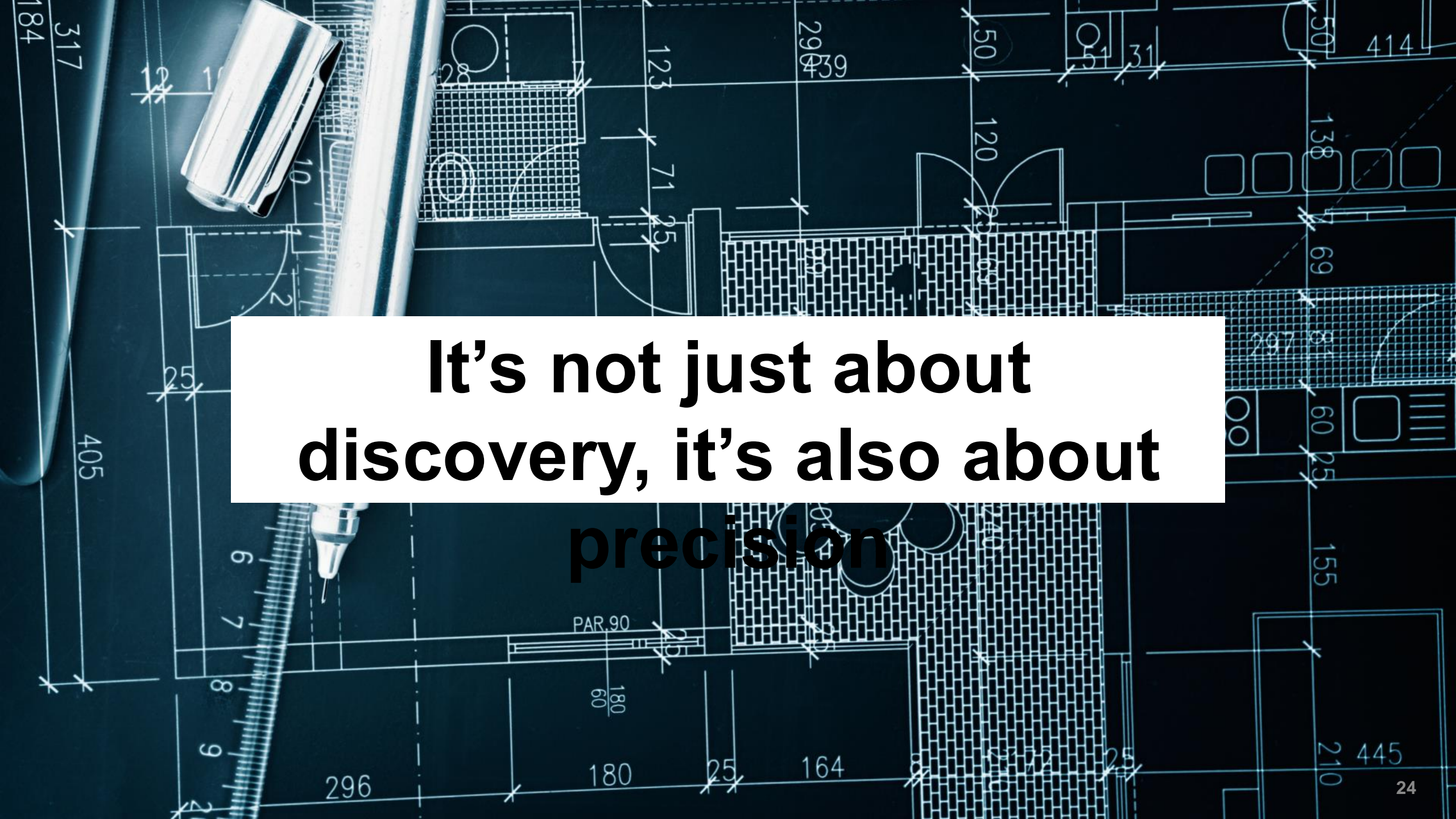
ATLAS

NEW PARTICLES



We haven't see them below this mass so far



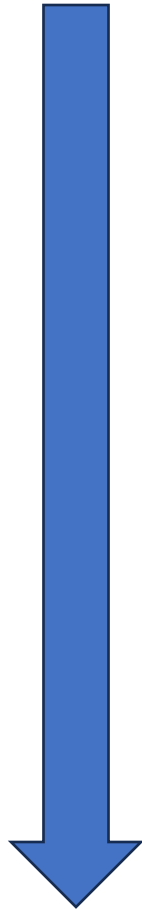
A top-down view of a drafting table with a blue-tinted background. The surface is covered with a complex architectural drawing in white lines, featuring various geometric shapes, grids, and dimension lines with numerical values. In the upper left, a silver mechanical pencil lies horizontally. In the lower left, a portion of a blue drafting triangle and a white ruler are visible. The overall scene conveys a sense of precision and technical work.

**It's not just about
discovery, it's also about
precision**

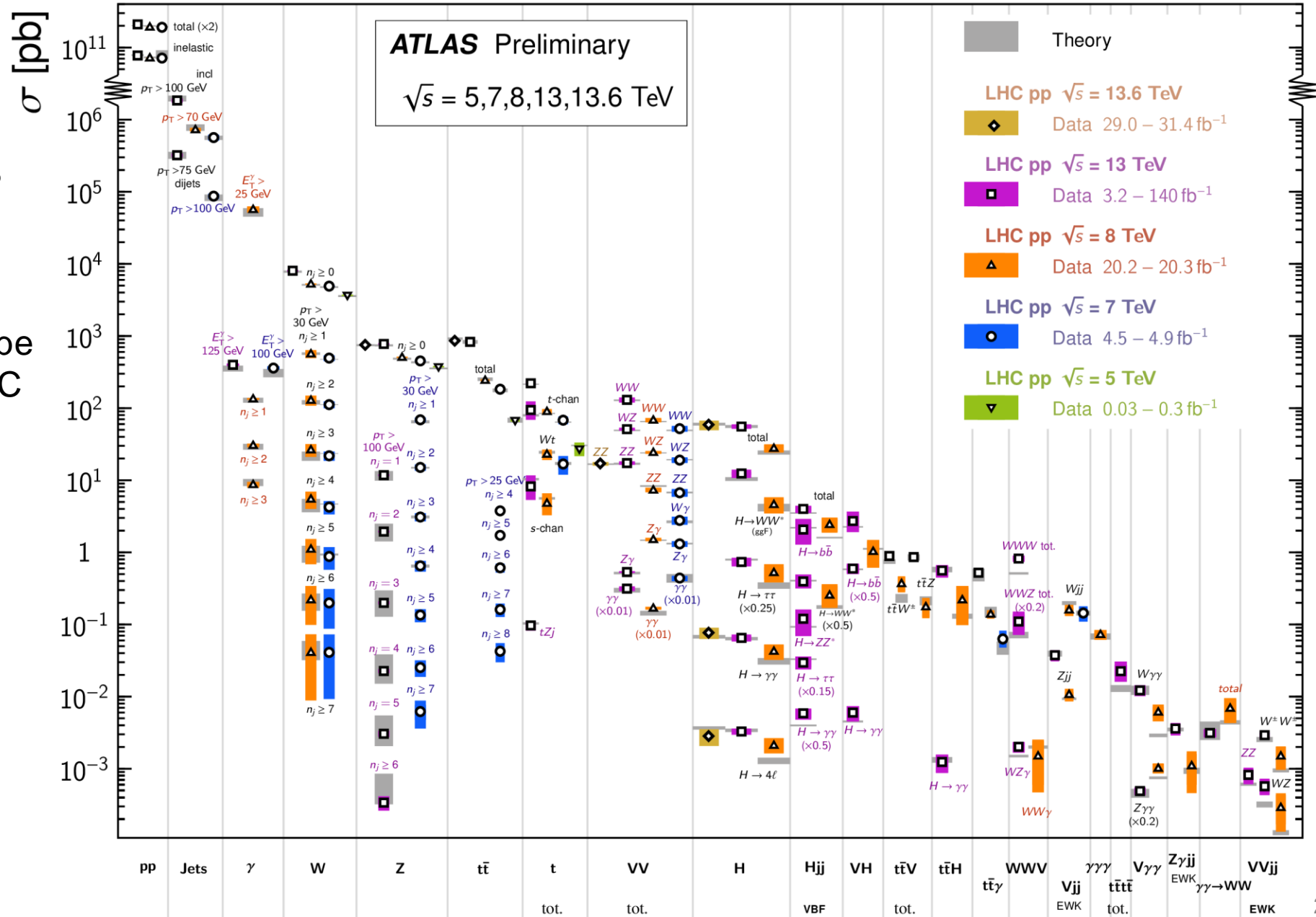
Standard Model Production Cross Section Measurements

Precision measurements

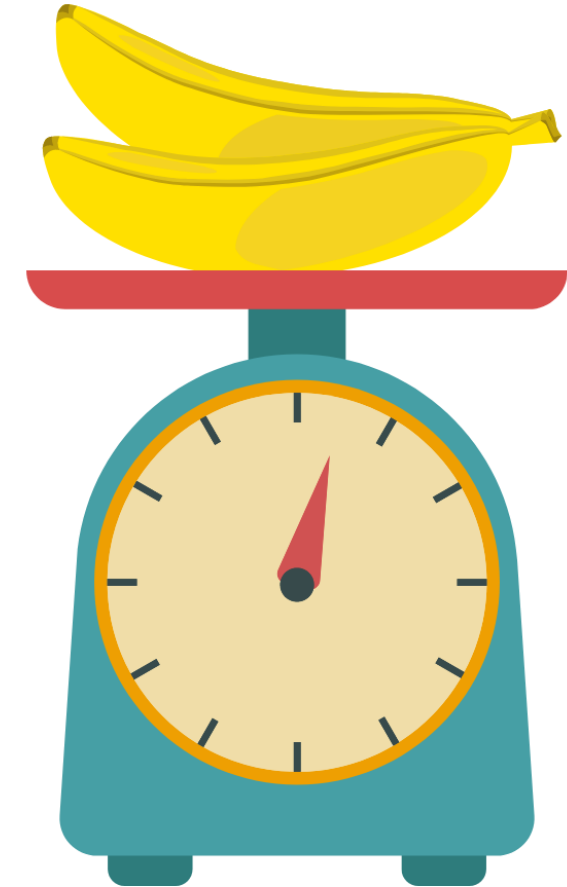
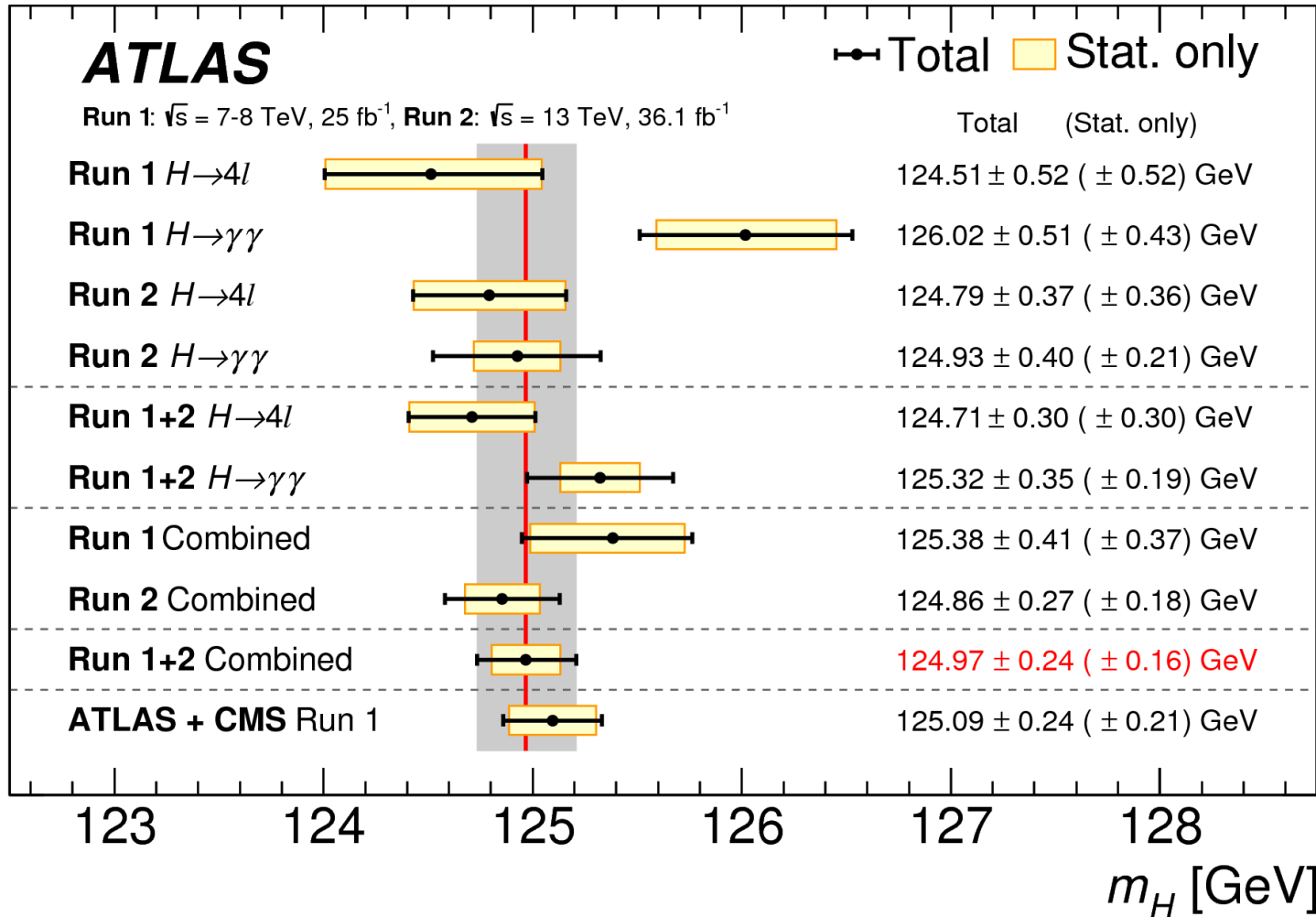
How likely a process is to be created in LHC collisions



A rarer process



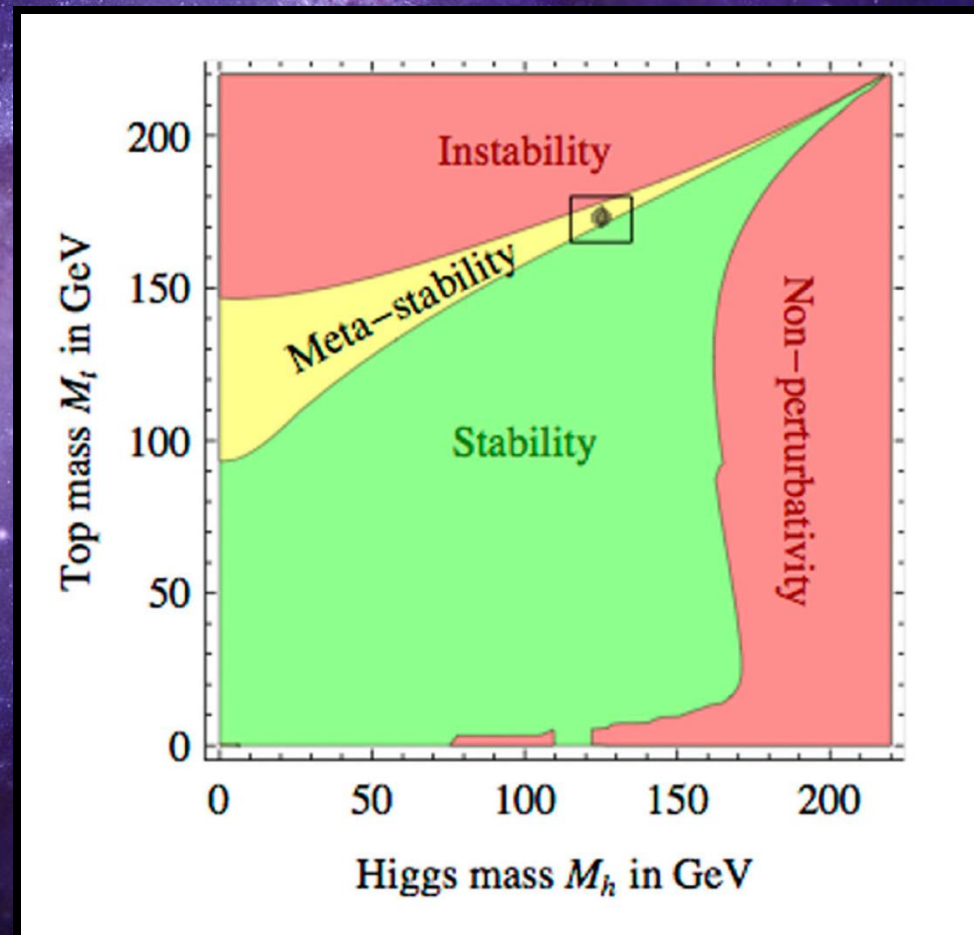
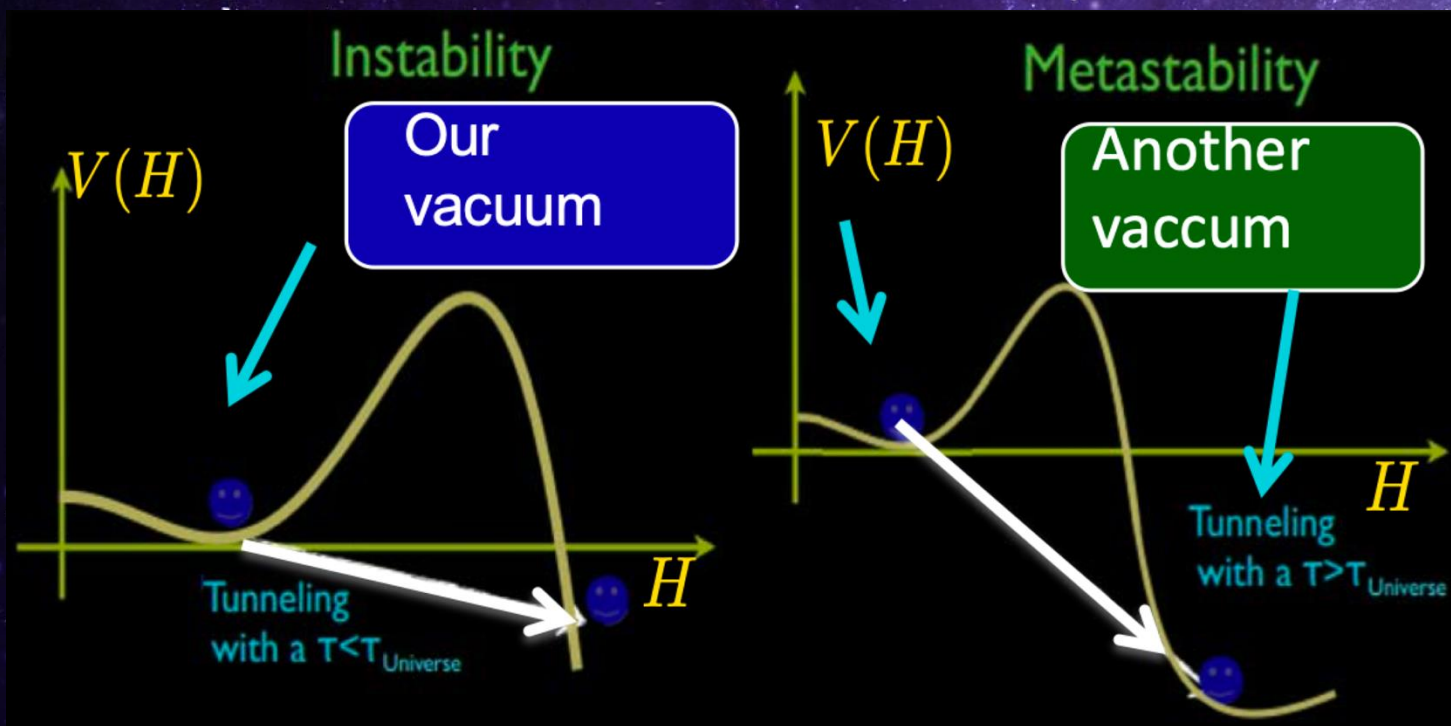
Precision Higgs measurements



Mass measurements

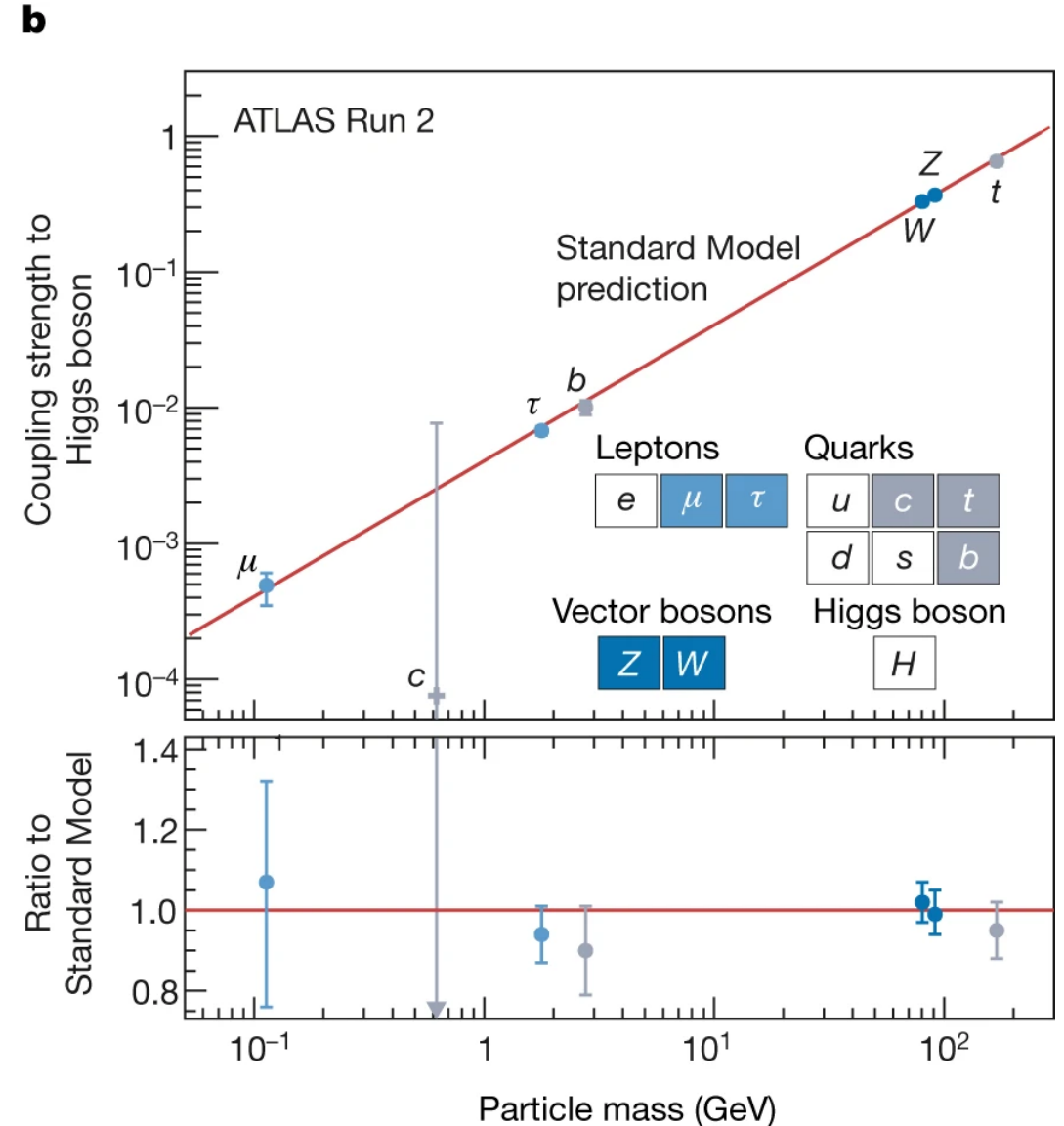
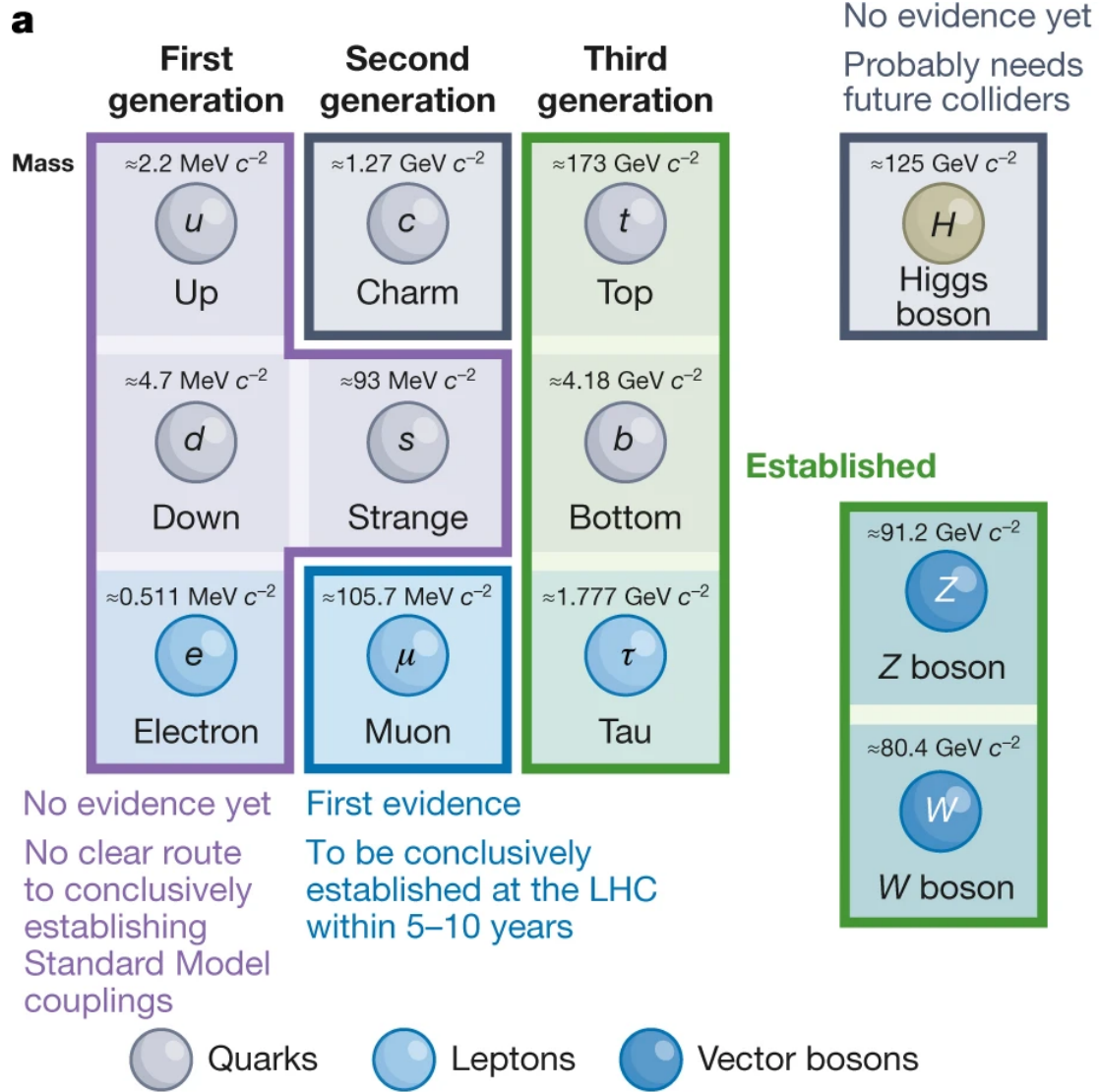
The stability of the universe depends on it!

(Please note: measuring this doesn't affect the stability. We're a passive observer.)



Precision Higgs measurements

Nature 607, p41-47 (2022), G. Salam et al.



Dark ?
matter

Next step: Higgs self-interaction



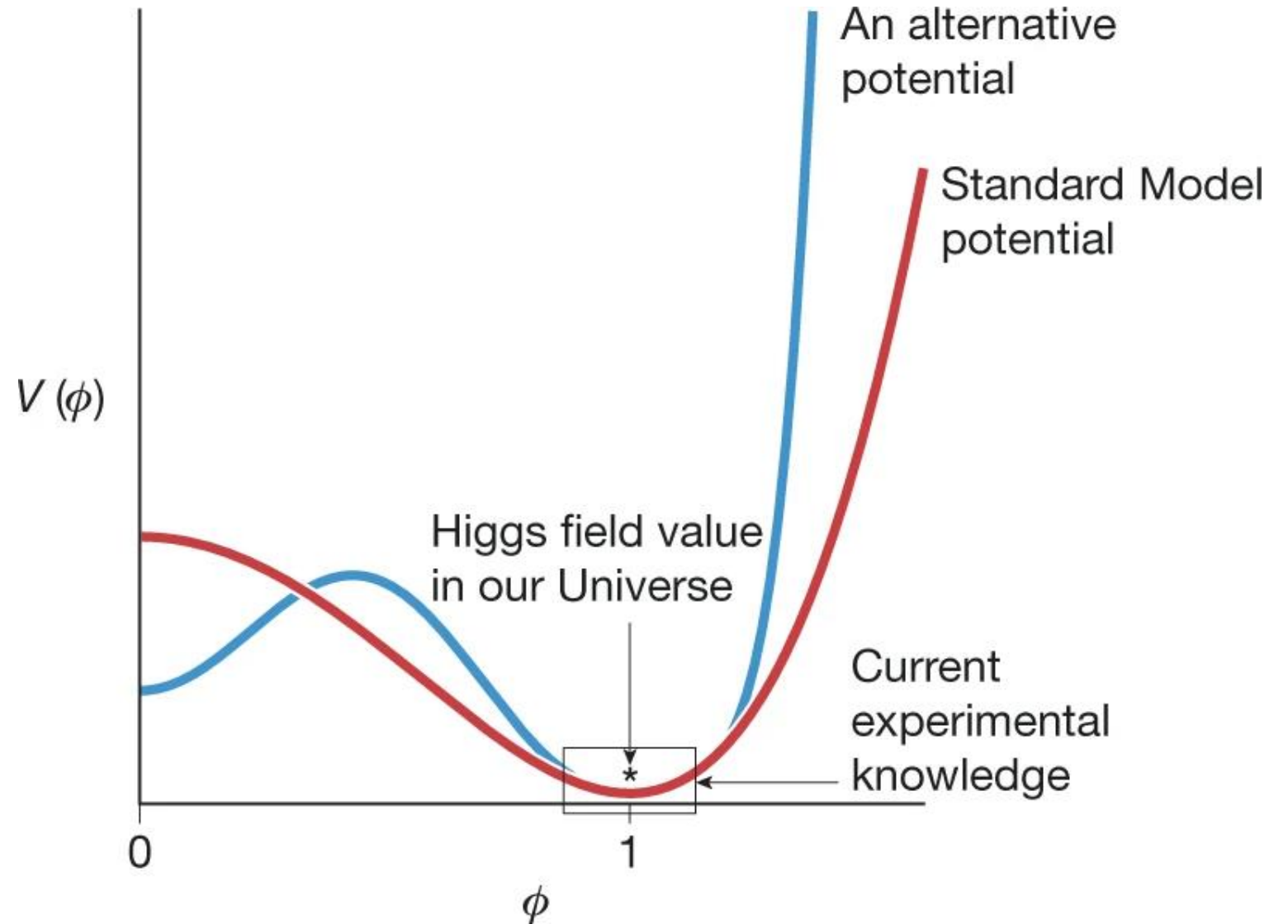
Hello there!

Image: Jorge Cham / PhD Comics

Nice to meet you!



Image: Jorge Cham / PhD Comics



**So how do we go
about answering
these questions?**

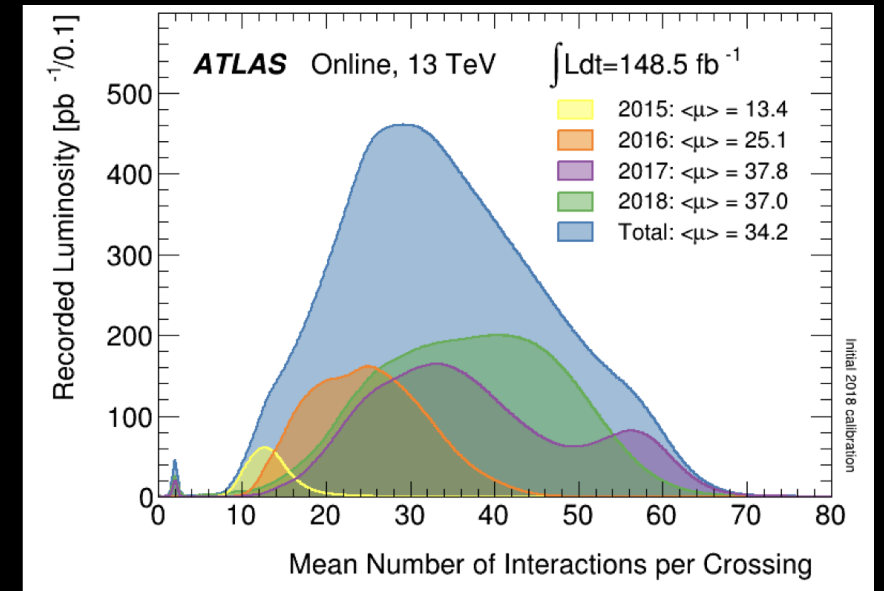
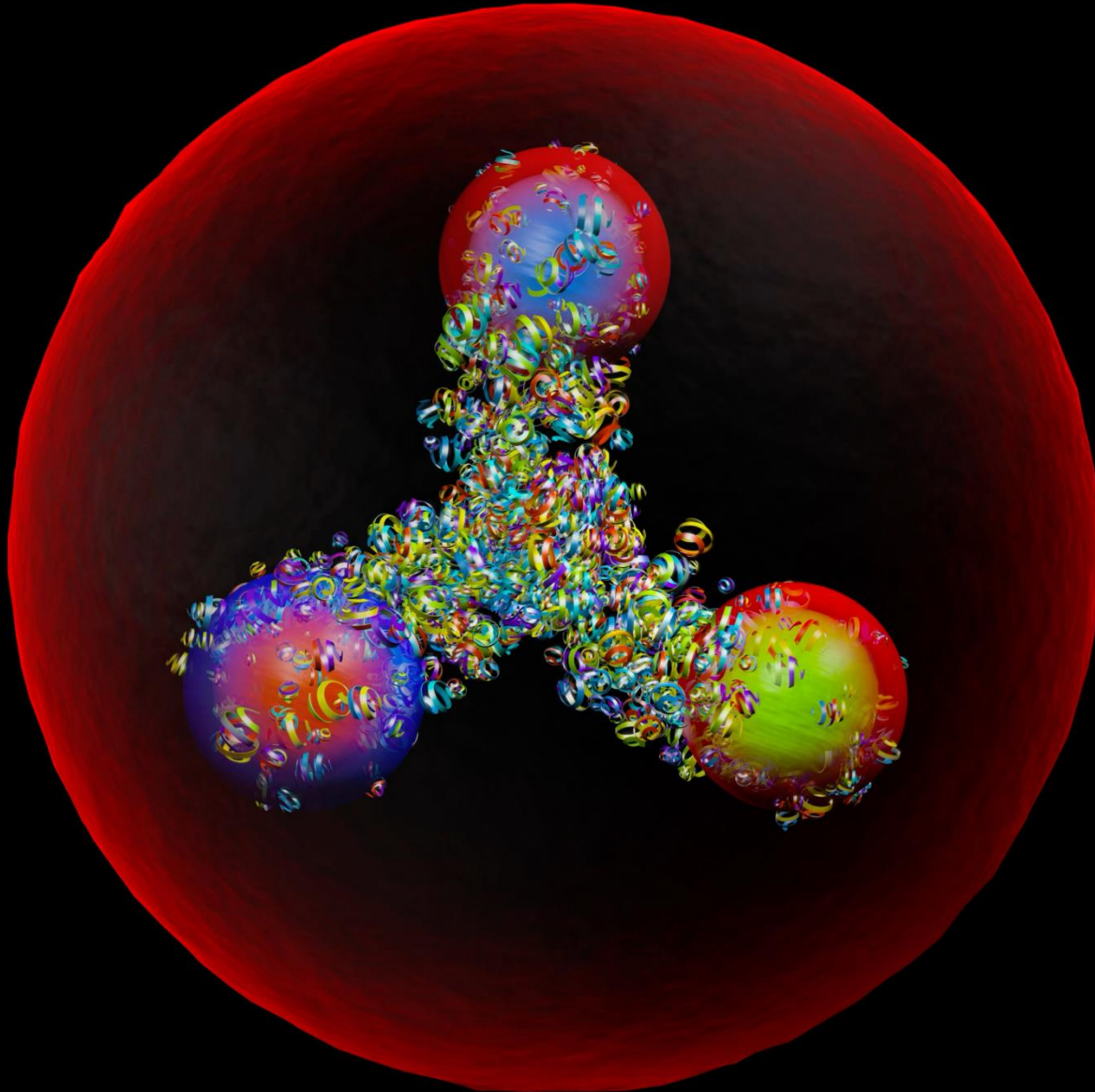


<https://videos.cern.ch/record/1750715>



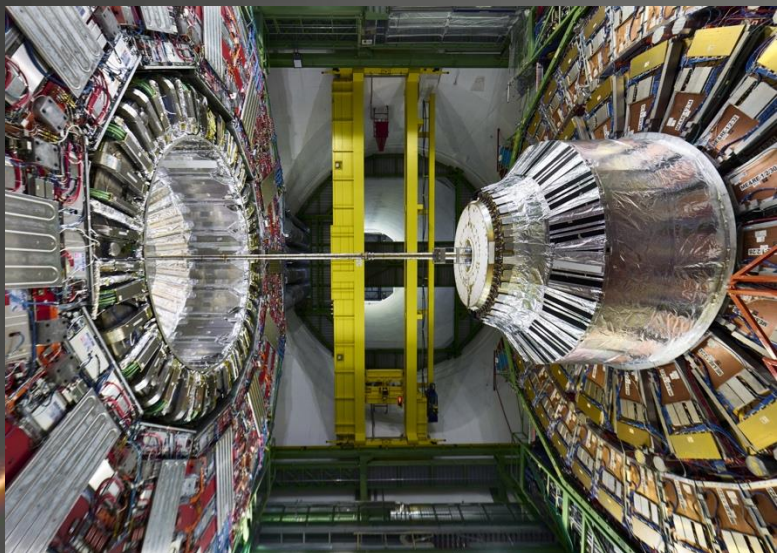
Accelerating Ylrrwln

Colliding protons



We wanted to explore a high range of masses: from 50 GeV to 1 TeV

The LHC detectors

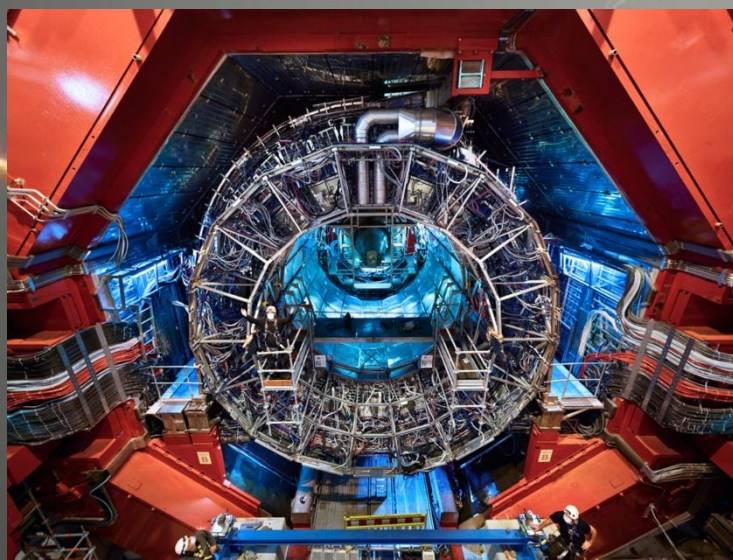


CMS

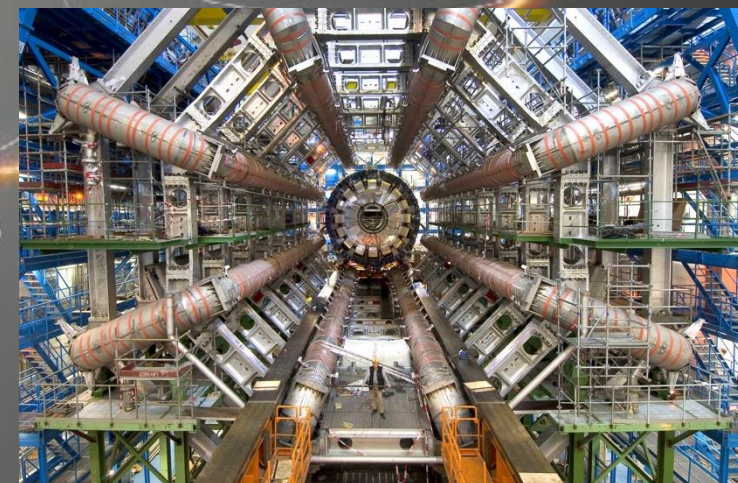


LHCb

<https://videos.cern.ch/record/1702939>



ALICE



ATLAS

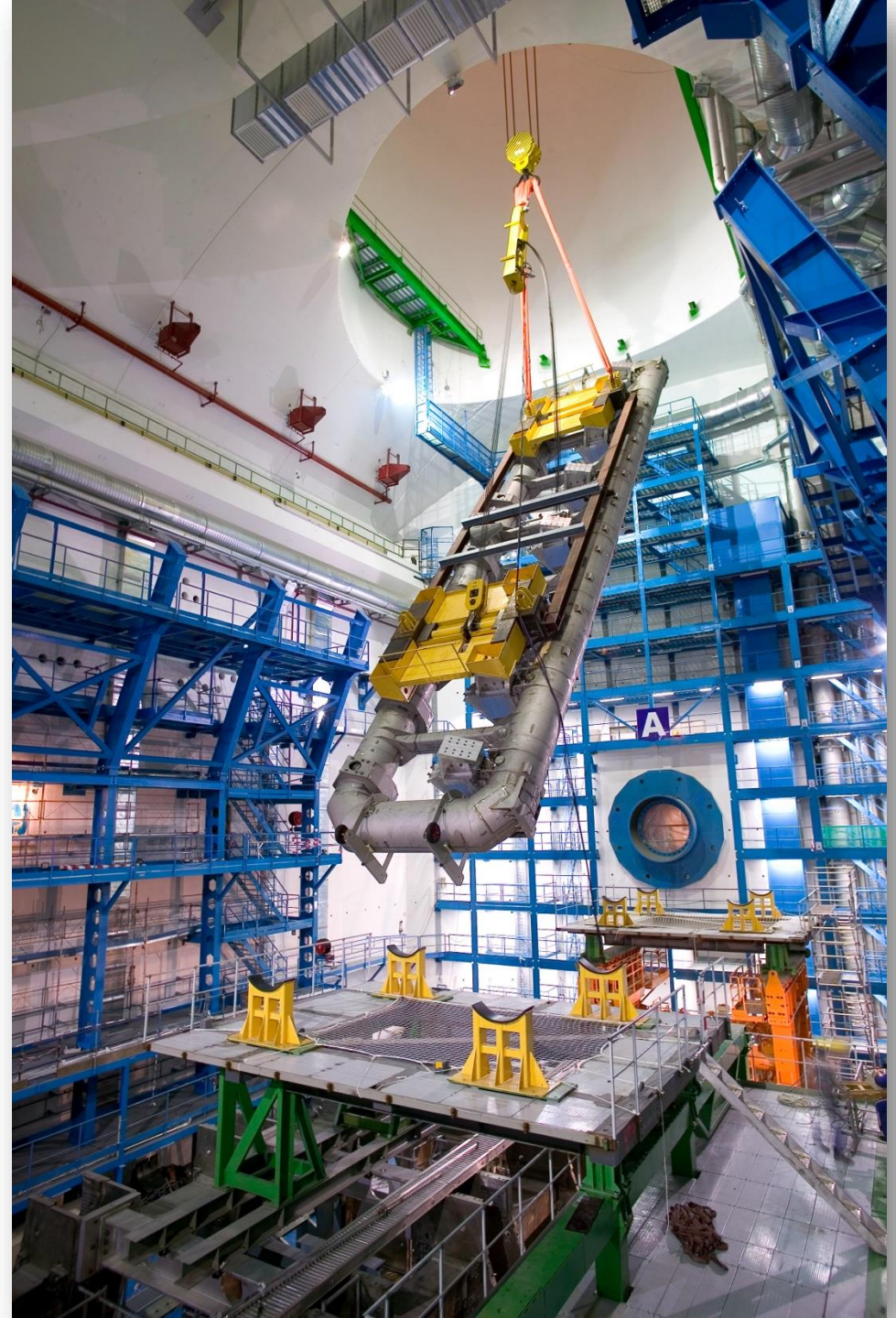
2002

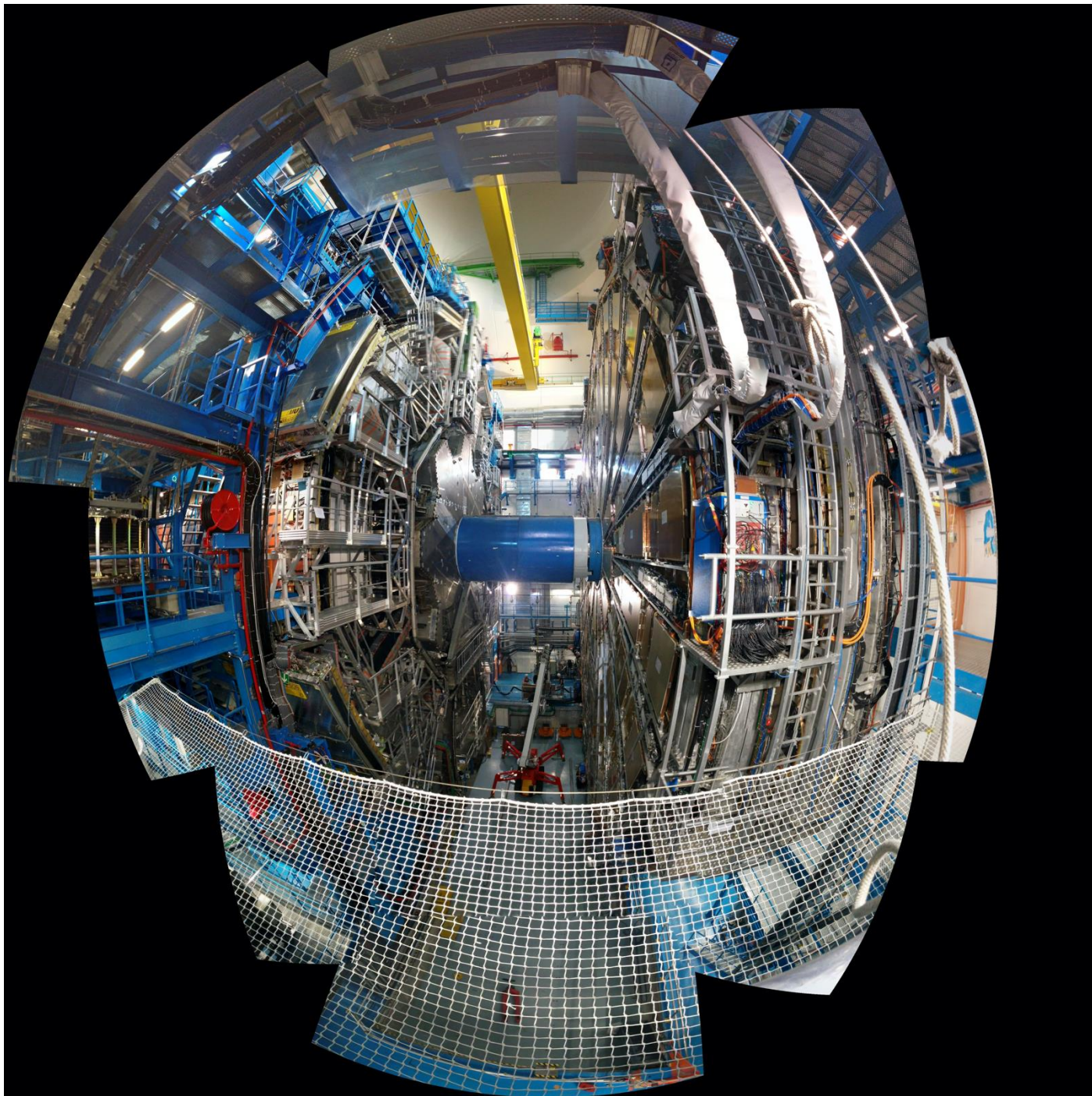
ATLAS Installation in the cavern

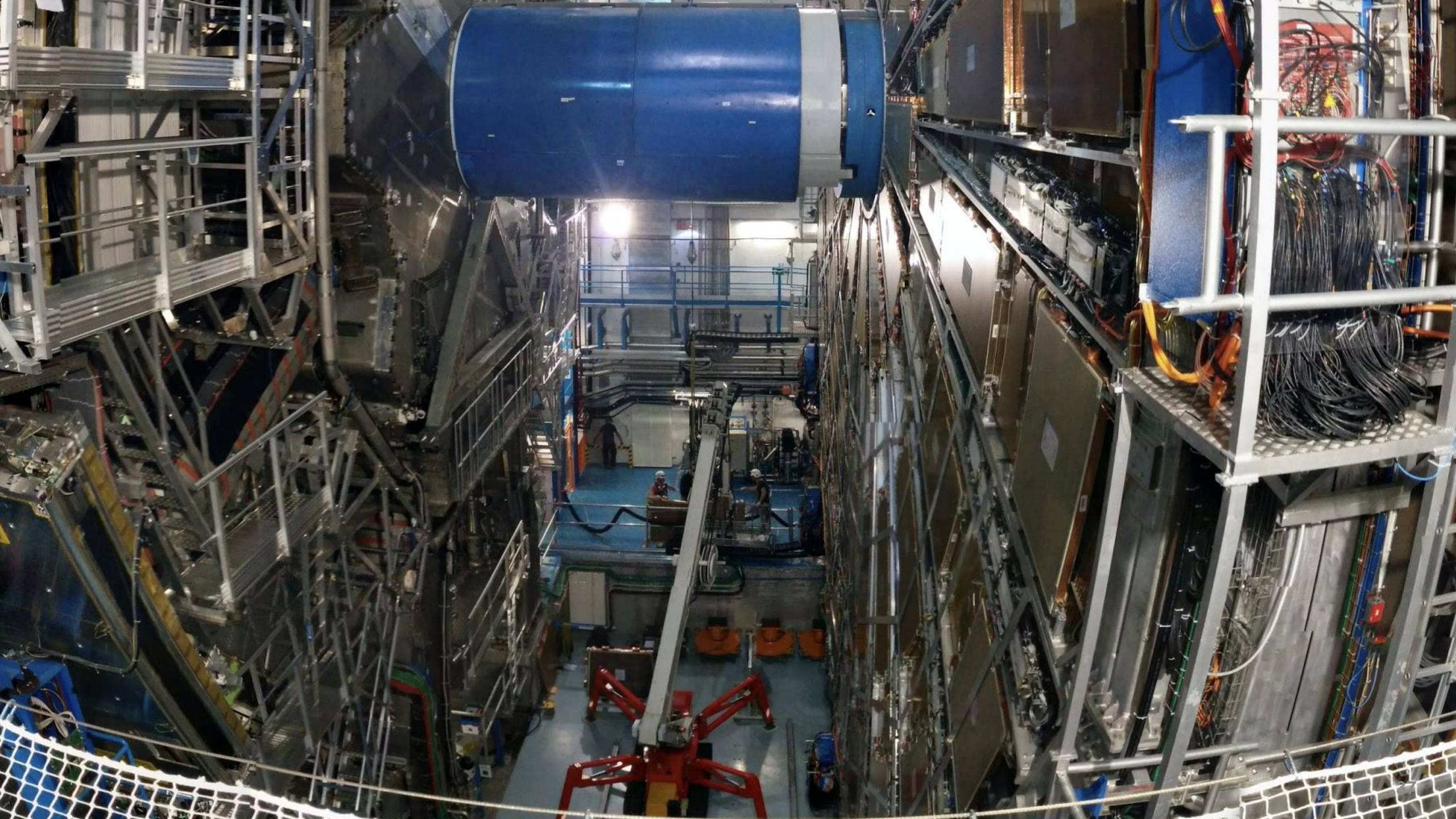


2004

ATLAS Installation in the cavern









- | | | |
|------------------------|-------------|--------------|
| Albania | Hong Kong | Peru |
| Algeria | Hungary | Philippines |
| Argentina | Iceland | Poland |
| Armenia | India | Portugal |
| Australia | Indonesia | Romania |
| Austria | Iran | Russia |
| Azerbaijan | Iraq | Saudi Arabia |
| Bangladesh | Ireland | Senegal |
| Belarus | Israel | Serbia |
| Belgium | Italy | Slovakia |
| Bosnia and Herzegovina | Japan | Slovenia |
| Botswana | Jordan | South Africa |
| Brazil | Kazakhstan | South Korea |
| Bulgaria | Kenya | Spain |
| Burundi | Kyrgyzstan | Sri Lanka |
| Canada | Latvia | Sudan |
| Chile | Lebanon | Swaziland |
| China | Lithuania | Sweden |
| Colombia | Luxembourg | Switzerland |
| Costa Rica | Madagascar | Syria |
| Croatia | Malaysia | Taiwan |
| Cuba | Malta | Thailand |
| Cyprus | Mauritius | Tunisia |
| Czech Republic | Mexico | Turkey |
| Denmark | Mongolia | Ukraine |
| Ecuador | Montenegro | UAE |
| Egypt | Morocco | UK |
| Finland | Nepal | USA |
| France | Netherlands | Uruguay |
| Georgia | New Zealand | Uzbekistan |
| Germany | Niger | Venezuela |
| Ghana | Nigeria | Vietnam |
| Greece | Norway | Zambia |
| Honduras | Pakistan | Zimbabwe |
| | Palestine | |

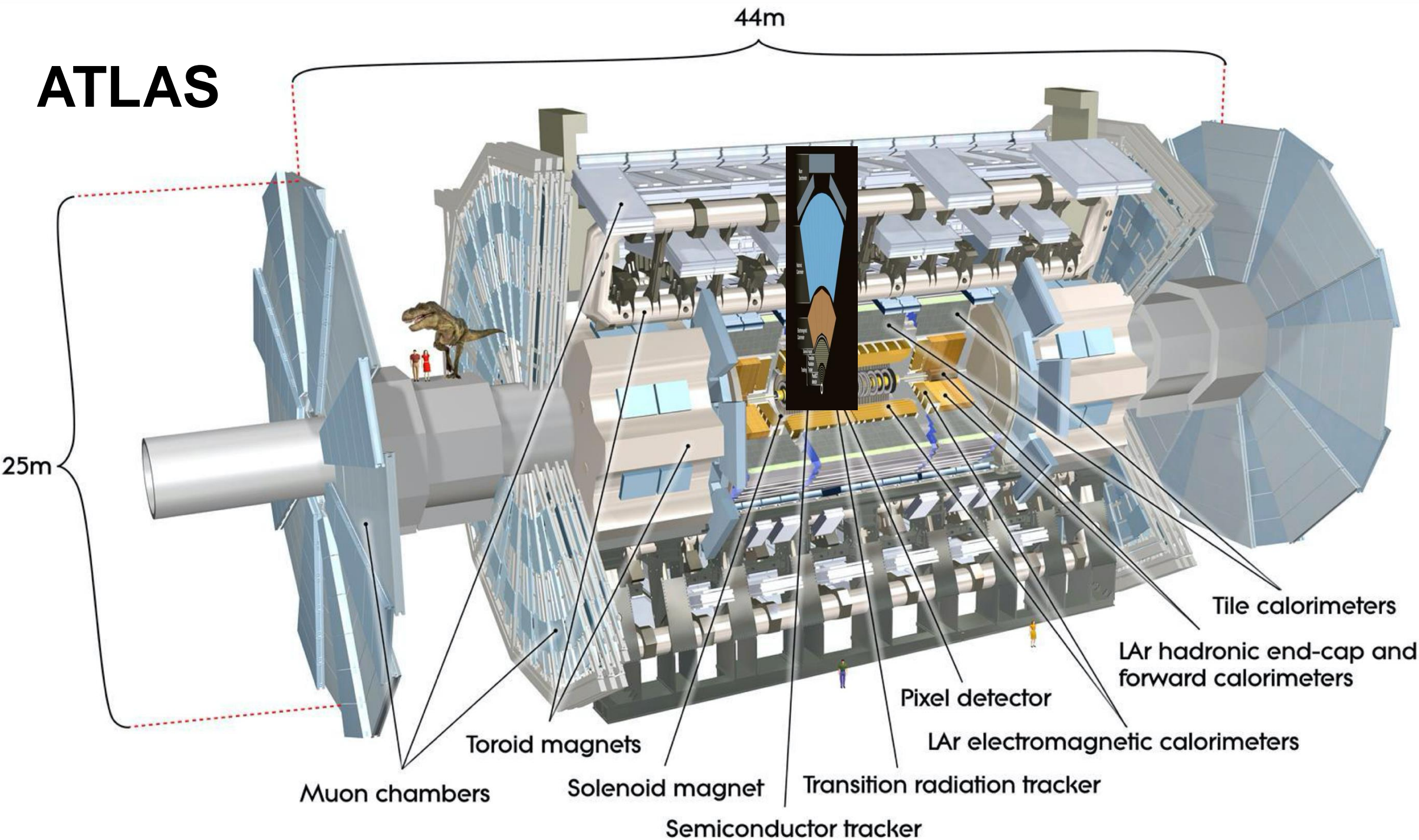
ATLAS Collaboration member nationalities

Over 5500 members of 103 nationalities





ATLAS



Muon Spectrometer

Measures muons

<https://videos.cern.ch/record/1458883>
(with very dramatic the music :D)

Hadronic Calorimeter

Measures the energy

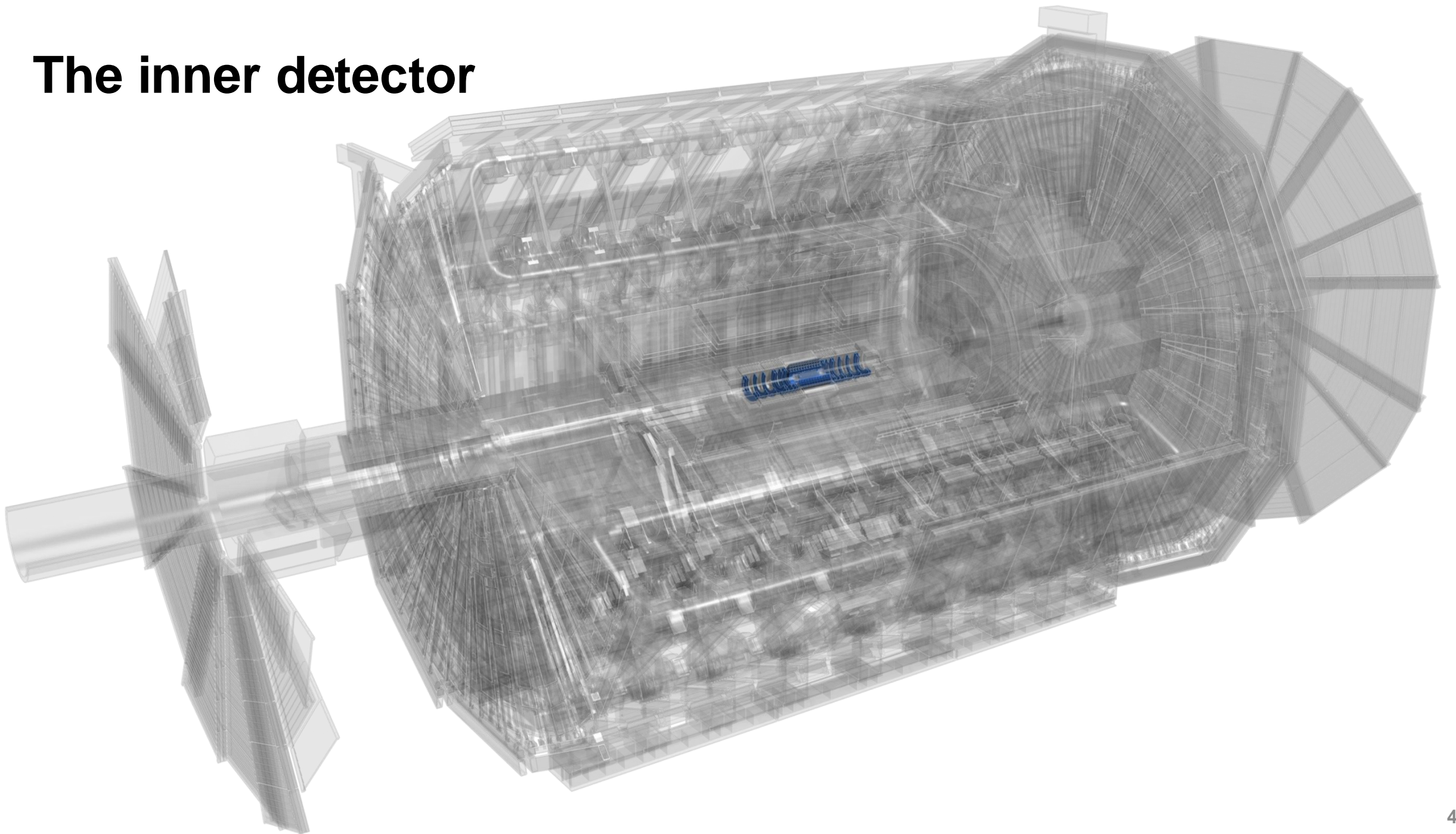
Electromagnetic Calorimeter

Solenoid magnet
Tracking { Transition Radiation Tracker
Pixel/SCT detector

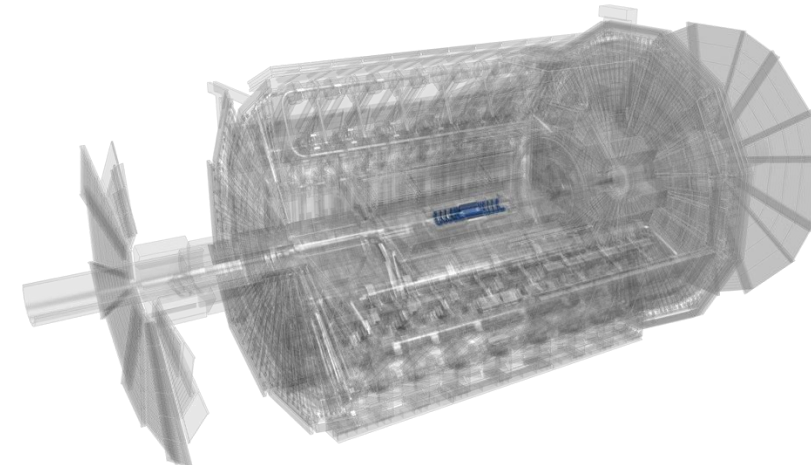
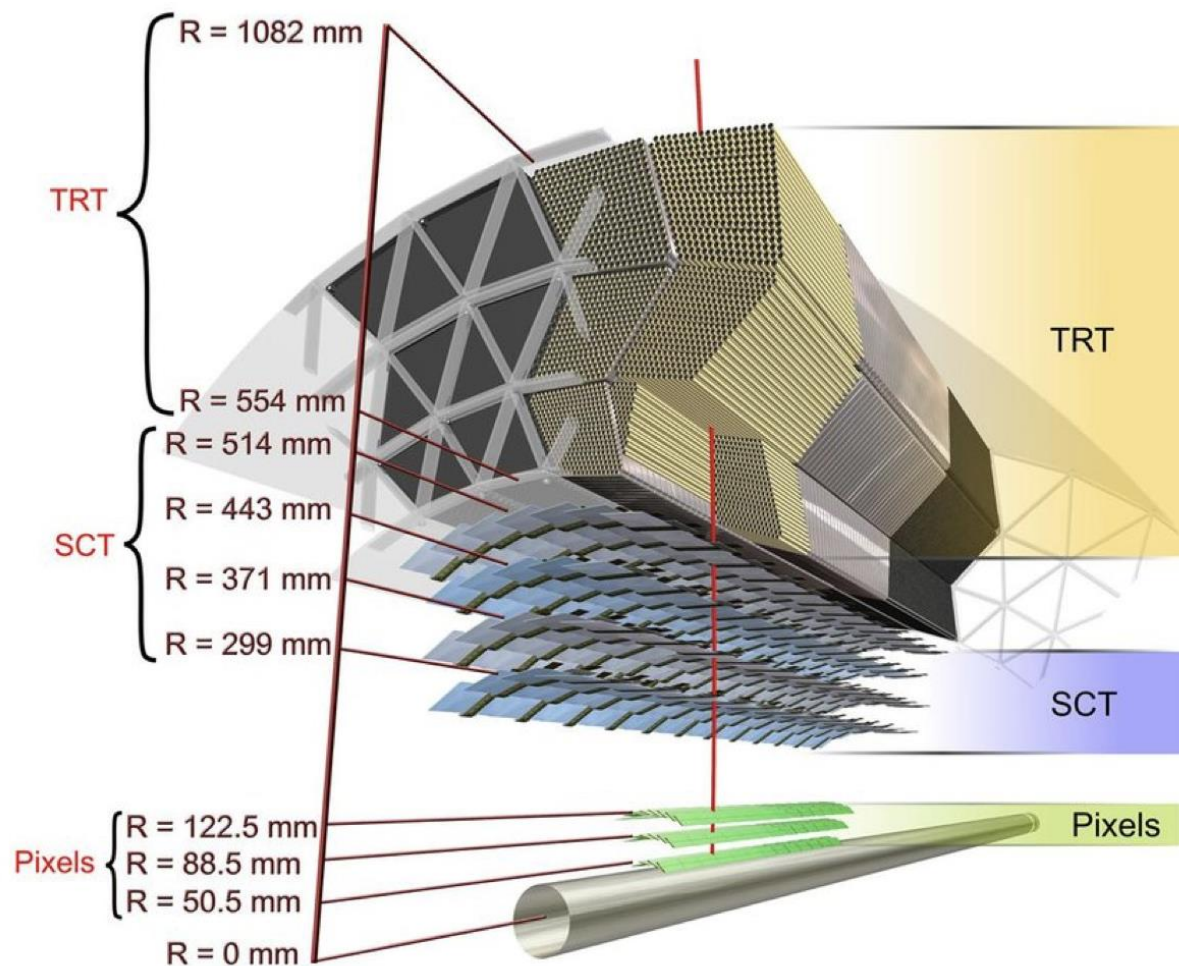
Tracks the path of charged particles

LHC beam pipe

The inner detector



The inner detector



THE INNER DETECTOR

The Inner Detector is the innermost part of ATLAS to see the decay products of the collisions, so it is very compact and highly sensitive. It consists of three different systems, measuring the direction, momentum and charge of electrically-charged particles produced in collisions.



PIXEL DETECTOR

Located just 3.3 cm from the LHC beam line, the Pixel Detector is the first point of detection in the ATLAS experiment. It is made up of four layers of silicon pixels, with each pixel smaller than a grain of sand. As charged particles burst out from the collision point, they leave behind small energy deposits in the Pixel Detector. These signals are measured with a precision of almost $10 \mu\text{m}$ to determine the origin and momentum of the particle. The Pixel Detector is incredibly compact, with over 92 million pixels and almost 2000 detector elements.



SEMICONDUCTOR TRACKER

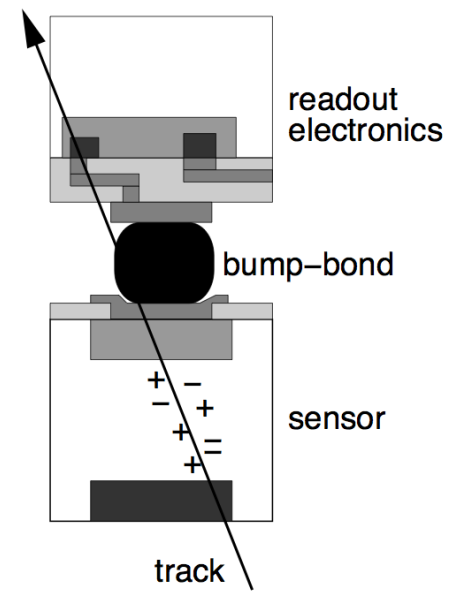
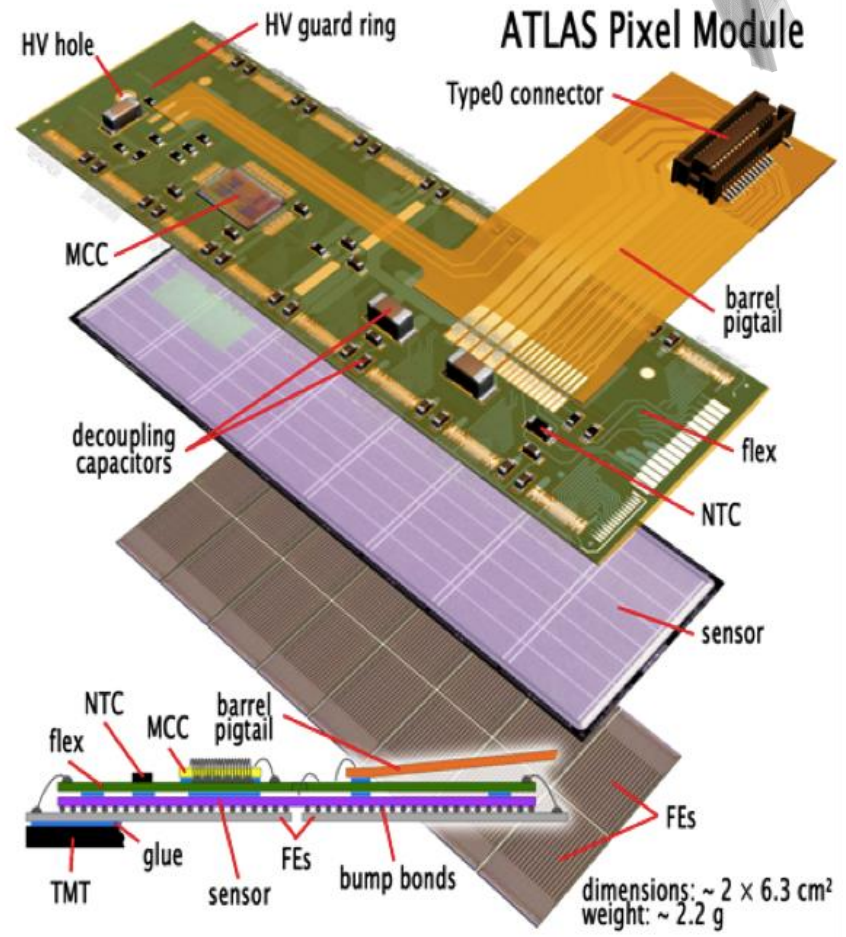
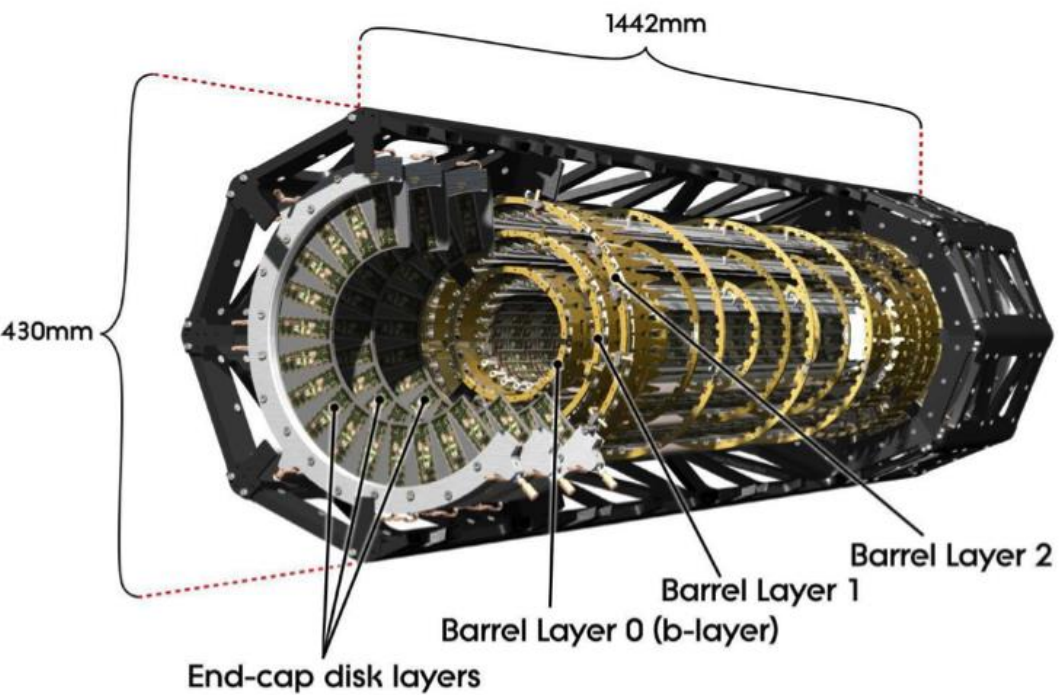
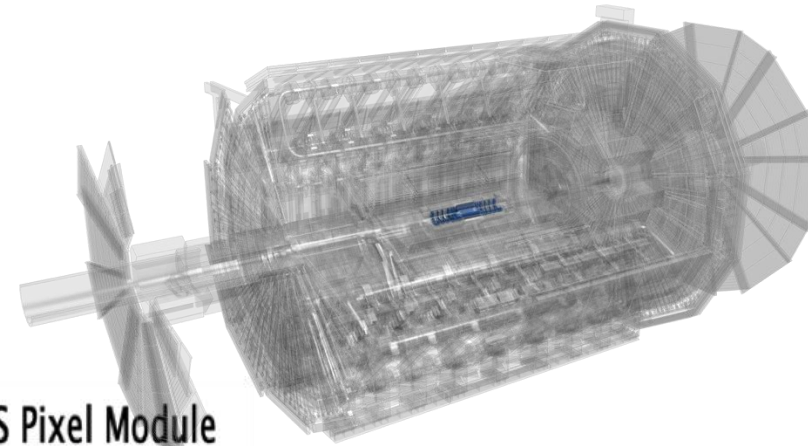
The Semiconductor Tracker surrounds the Pixel Detector and is used to detect and reconstruct the tracks of charged particles produced during collisions. It consists of over 4,000 modules of 6 million "micro-strips" of silicon sensors. Its layout is optimised such that each particle crosses at least four layers of silicon. This allows scientists to measure particle tracks with a precision of up to $25 \mu\text{m}$ - that's less than half the width of a human hair!



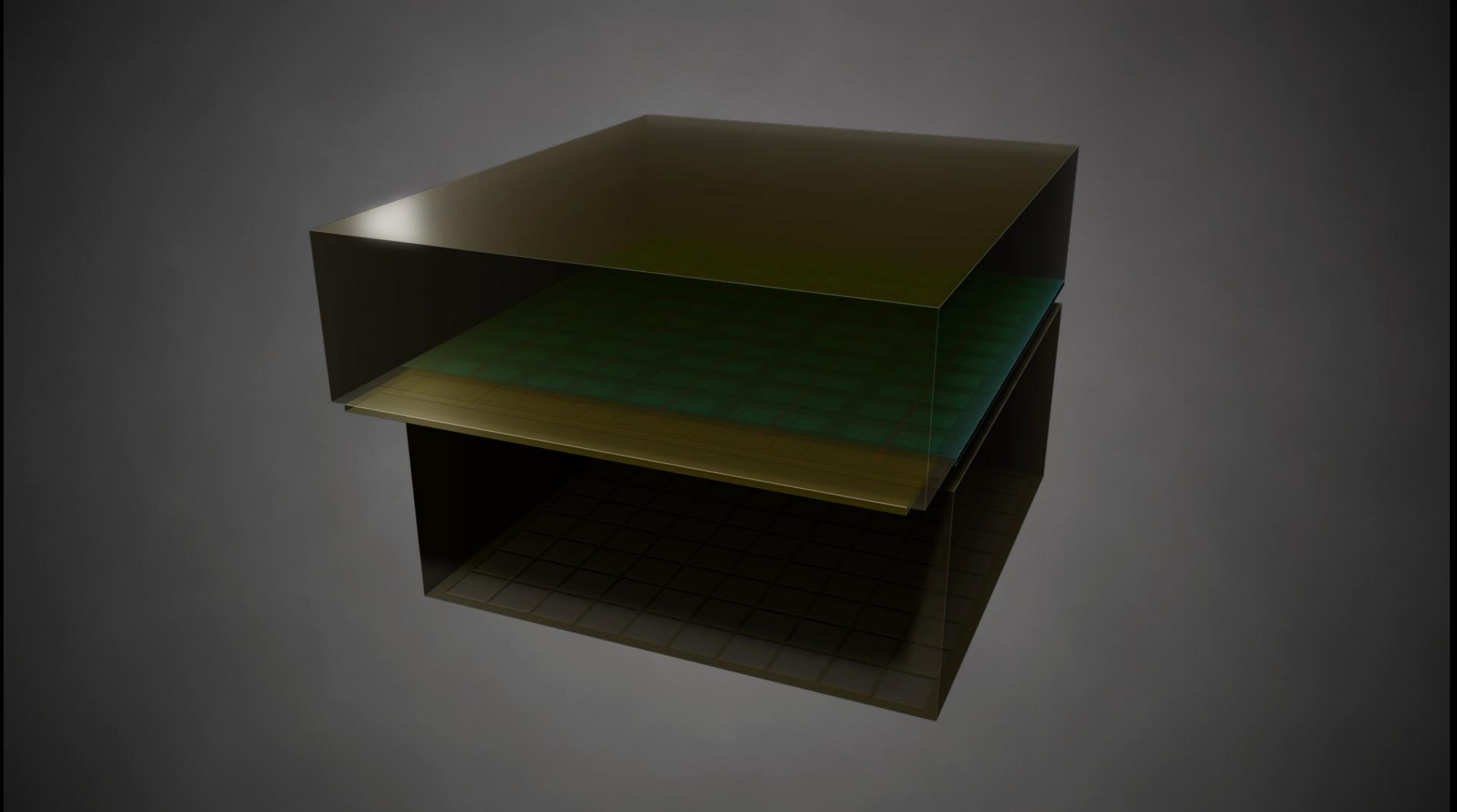
TRANSITION RADIATION TRACKER

The third and final layer of the Inner Detector is the Transition Radiation Tracker (TRT). Unlike its neighbouring sub-detectors, the TRT is made up of 300,000 thin-walled drift tubes (or "straws"). Each straw is just 4 mm in diameter, with a $30 \mu\text{m}$ gold-plated tungsten wire in its centre. The straws are filled with a gas mixture. As charged particles cross through the straws, they ionise the gas to create a detectable electric signal. This is used to reconstruct their tracks and, owing to the so-called transition radiation, provides information on the particle type that flew through the detector, i.e. if it is an electron or pion.

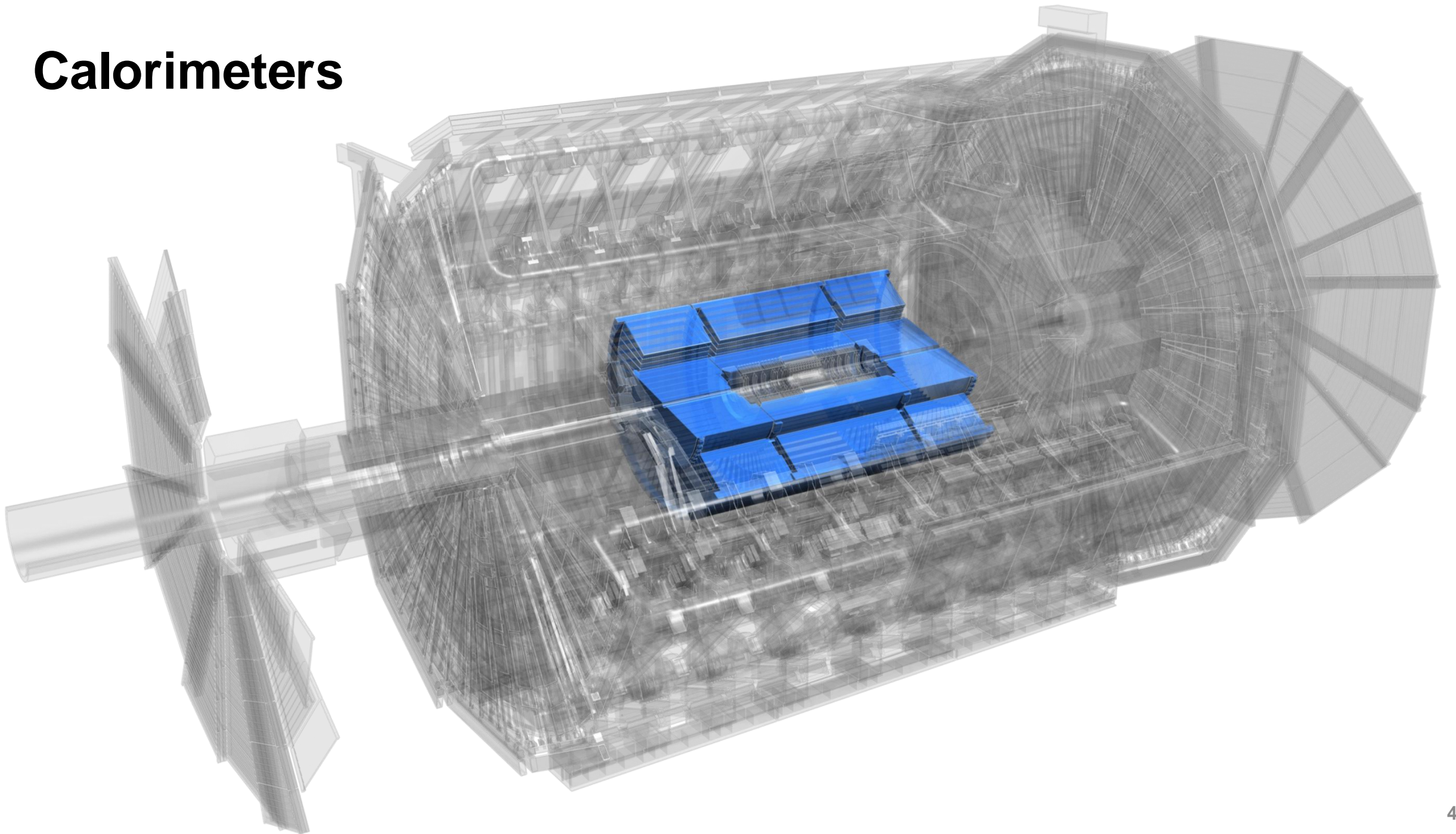
The pixel detector



How a pixel detector works

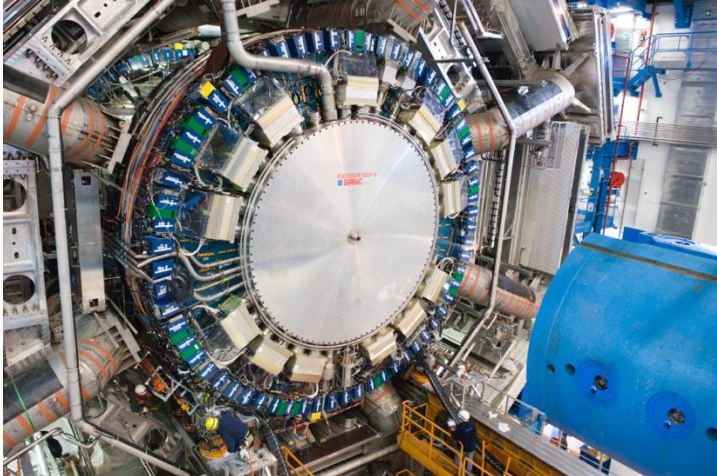
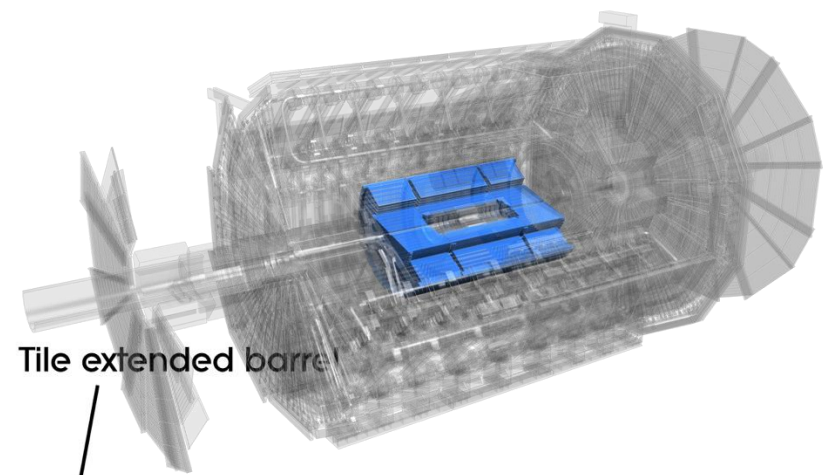


Calorimeters



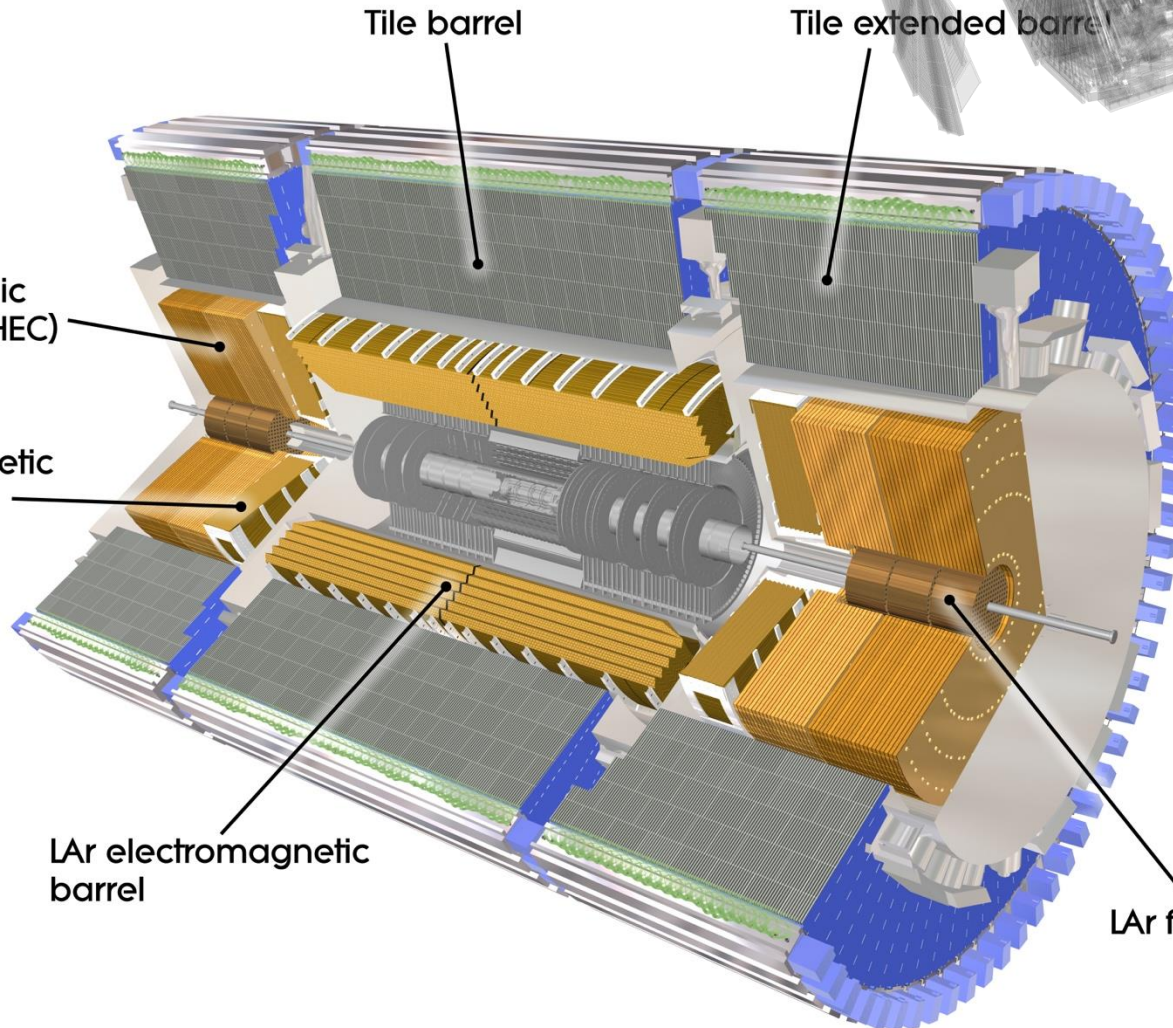
Calorimeters

Information sheets:
<https://atlas.cern/Resources/Fact-sheets>



LAr hadronic end-cap (HEC)

LAr electromagnetic end-cap (EMEC)



CALORIMETERS

Calorimeters measure the energy of particles created in high-energy LHC collisions. They are designed to absorb most of the particles coming from a collision, forcing them to deposit all of their energy and stop within the detector. ATLAS calorimeters consist of layers of an "absorbing" high-density material that stops incoming particles, interleaved with layers of an "active" medium that measures their energy.

LIQUID ARGON CALORIMETER

The Liquid Argon (LAr) Calorimeter surrounds the ATLAS Inner Detector and measures the energy of electrons, photons and hadrons. It features layers of metal (either tungsten, copper or lead) that absorb incoming particles, converting them into a "shower" of new, lower energy particles. These particles ionize liquid argon sandwiched between the layers, producing an electric current that is measured. By combining all of the detected currents, physicists can determine the energy of the original particle that hit the detector.

The central region of the calorimeter is specially designed to identify electrons and photons. It features a characteristic accordion structure, with a honeycomb pattern, to ensure that no particle escapes unchallenged.

To keep the argon in liquid form, the calorimeter is kept at -184 °C. Specially-designed, vacuum-sealed cylinders of cables bring the electronic signals from the cold liquid argon to the warm area where the readout electronics are located.

TILE HADRONIC CALORIMETER

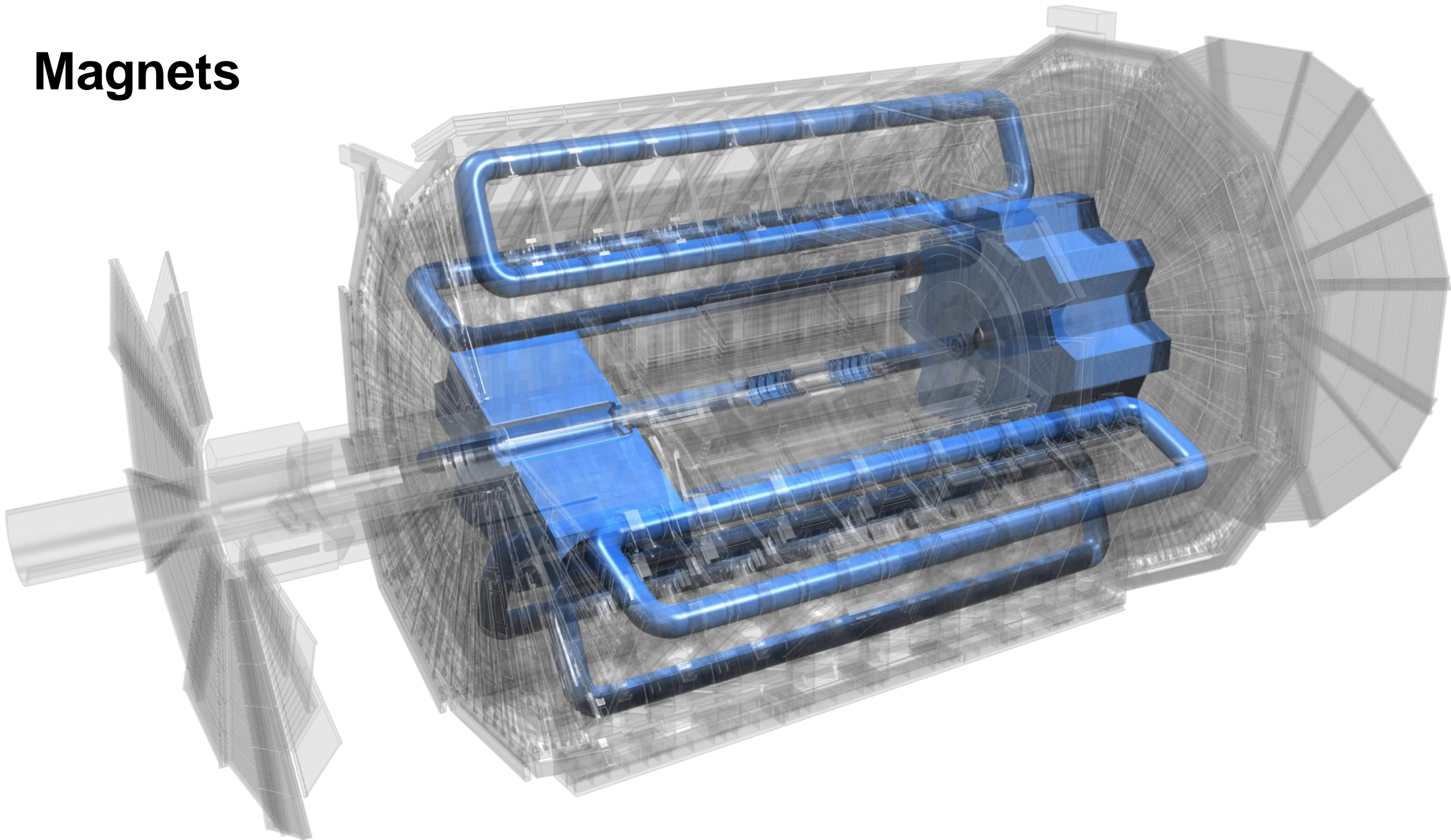
The Tile Calorimeter surrounds the LAr calorimeter and measures the energy of hadronic particles, which do not deposit all of their energy in the LAr Calorimeter. It is made of layers of steel and plastic scintillating tiles. As particles hit the layers of steel, they generate a shower of new particles. The plastic scintillators in turn produce photons, which are converted into an electric current whose intensity is proportional to the original particle's energy.

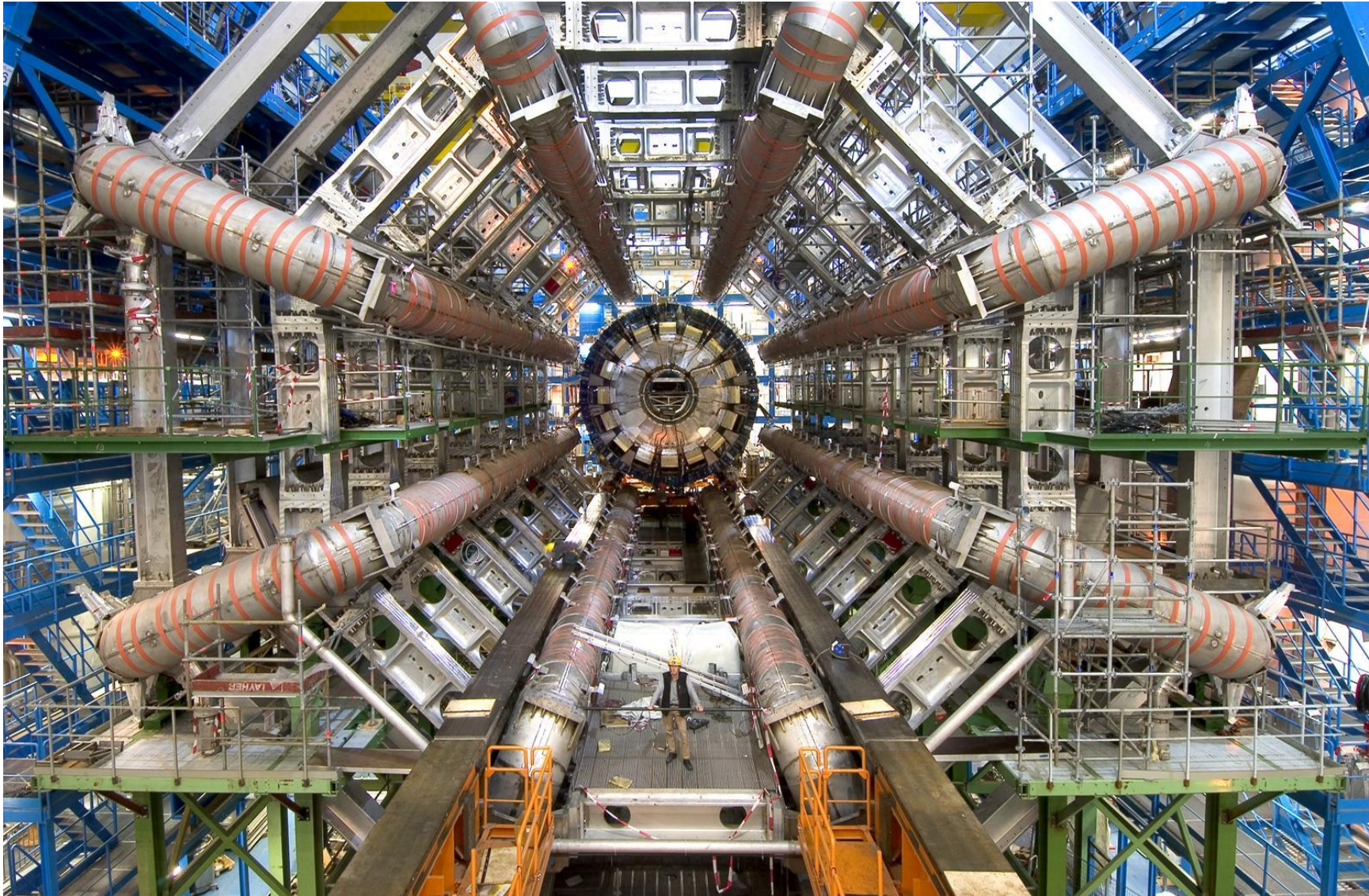
The Tile Calorimeter is made up of about 420,000 plastic scintillator tiles working in sync. It is the heaviest part of the ATLAS experiment, weighing almost 2900 tons!

<https://atlas.cern>

ATLAS EXPERIMENT

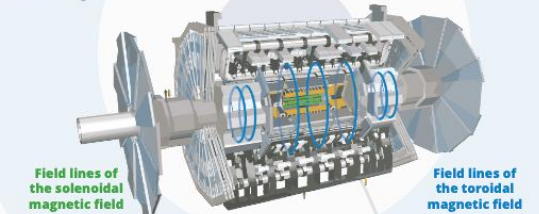
Magnets





MAGNET SYSTEM

ATLAS uses two different types of superconducting magnet systems – solenoidal and toroidal. When cooled to about 4.5 K (-268°C), these are able to provide strong magnetic fields that bend the trajectories of charged particles. This allows physicists to measure their momentum and charge.



CENTRAL SOLENOID MAGNET

The ATLAS solenoid surrounds the inner detector at the core of the experiment. This powerful magnet is 5.6 m long, 2.56 m in diameter and weighs over 5 tonnes. It provides a 2 Tesla magnetic field in just 4.5 cm thickness. This is achieved by embedding over 9 km of niobium-titanium superconductor wires into strengthened, pure aluminum strips, thus minimising possible interactions between the magnet and the particles being studied.

TOROID MAGNET

The ATLAS toroids use a series of eight coils to provide a magnetic field of up to 3.5 Tesla, used to measure the momentum of muons. There are three toroid magnets in ATLAS: two at the ends of the experiment, and one massive toroid surrounding the centre of the experiment.

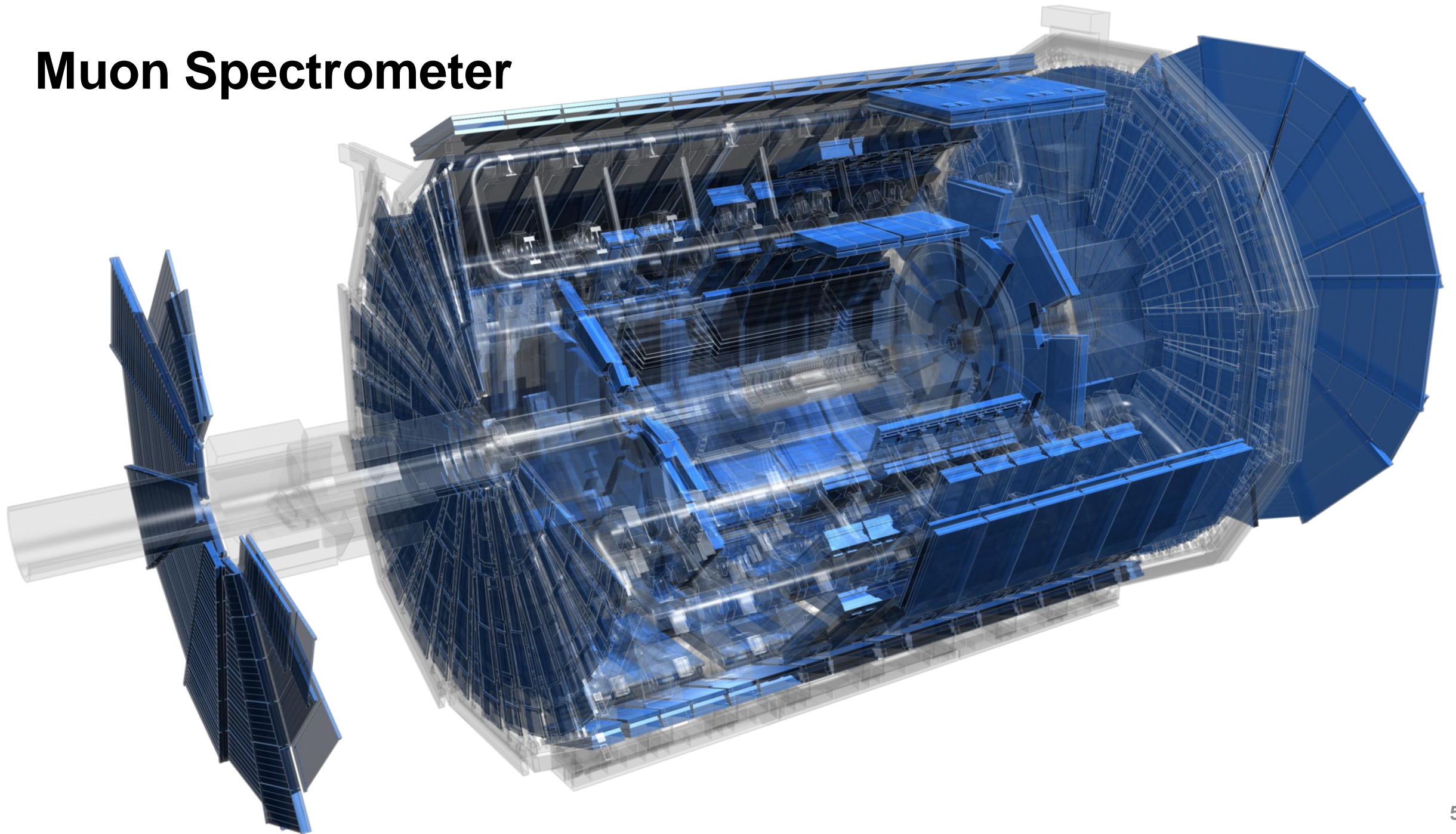
At 25.3 m in length, the central toroid is the largest toroidal magnet ever constructed and is an iconic element of ATLAS. It uses over 56 km of superconducting wire and weighs about 830 tonnes. The end-cap toroids extend the magnetic field to particles leaving the detector close to the beam pipe. Each end-cap is 10.7 m in diameter and weighs 240 tonnes.



<https://atlas.cern>

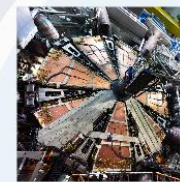
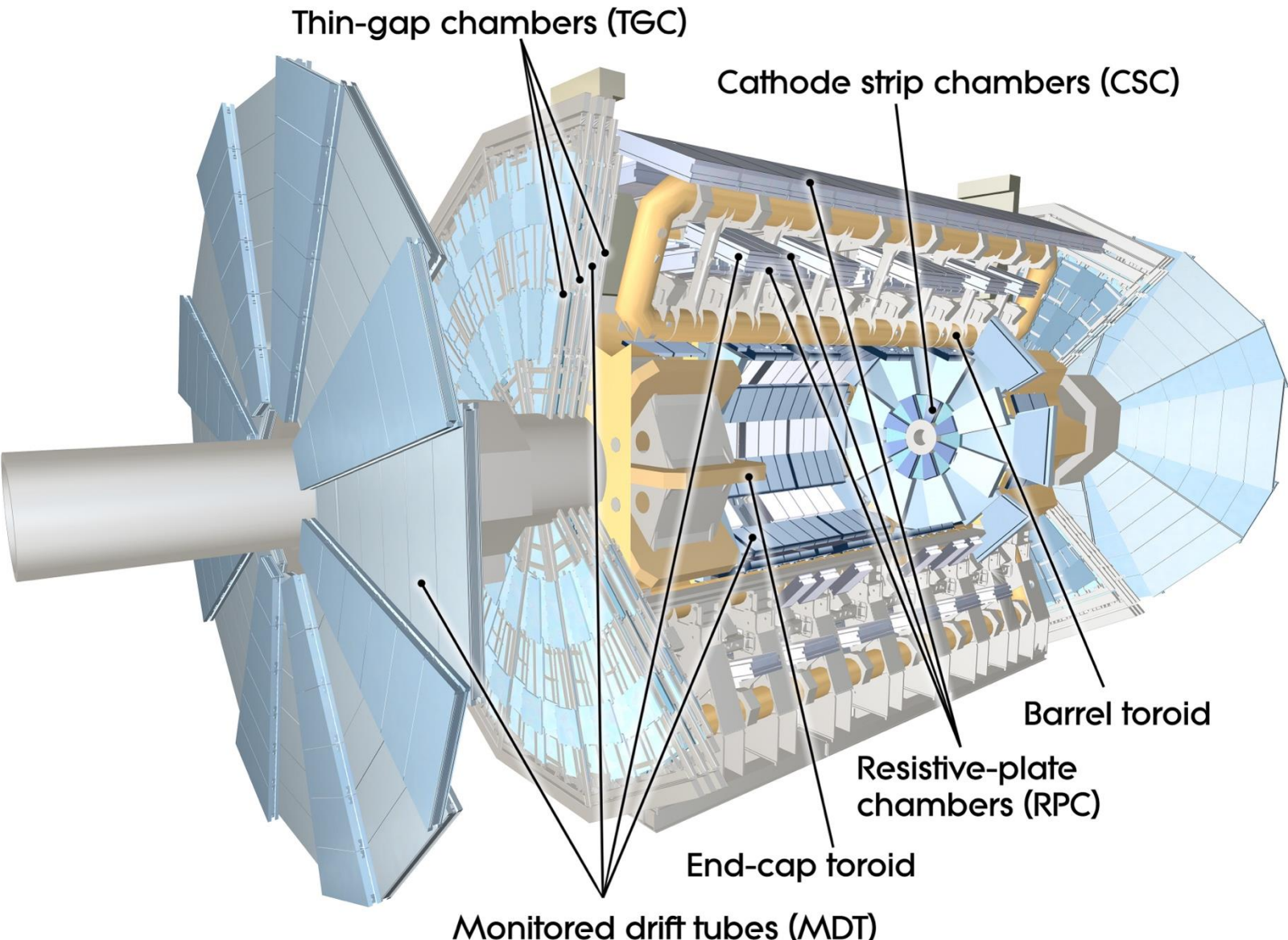
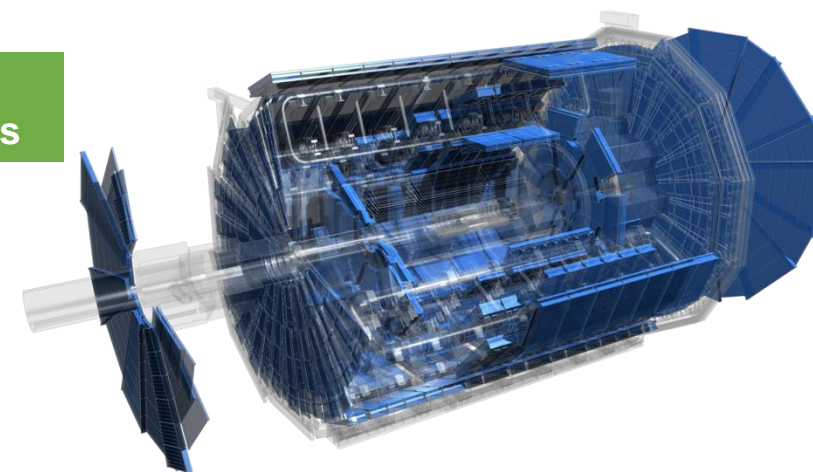


Muon Spectrometer



Muon Spectrometer

Information sheets:
<https://atlas.cern/Resources/Fact-sheets>



MUON SPECTROMETER

The outer layer of the ATLAS experiment is made of muon detectors. They identify and measure the momenta of muons - particles similar to electrons but 200 times heavier, which allows them to cross the thick calorimeter layers.

PRECISION DETECTORS

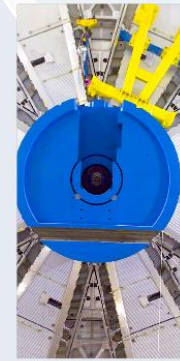
The precision detectors of the Muon Spectrometer are able to determine the position of a muon, to an accuracy of less than a 10th of a millimeter!



Monitored Drift Tube (MDTs) detectors are composed of 3 cm wide aluminum tubes filled with a gas mixture. Muons pass through the tubes, knocking electrons out of the gas. These then drift to a wire at the tube's centre to induce a signal. Over 380,000 aluminum tubes are stacked up in several layers in order to precisely trace the trajectory of each muon.

FAST-RESPONSE DETECTORS

ATLAS uses fast-response detectors to quickly select collision events that are potentially interesting for physics analysis. They make this decision within 2.5 μ s (400,000th of a second).



The Resistive Plate Chambers (RPCs) surround the central region of the ATLAS experiment. They consist of pairs of parallel plastic plates at an electric potential difference, separated by a gas volume. Thin Gap Chambers (TGCs) are found at the ends of the ATLAS experiment and consist of parallel 30 μ m wires in a gas mixture. Both chambers detect muons when they ionise the gas mixture and generate a signal.

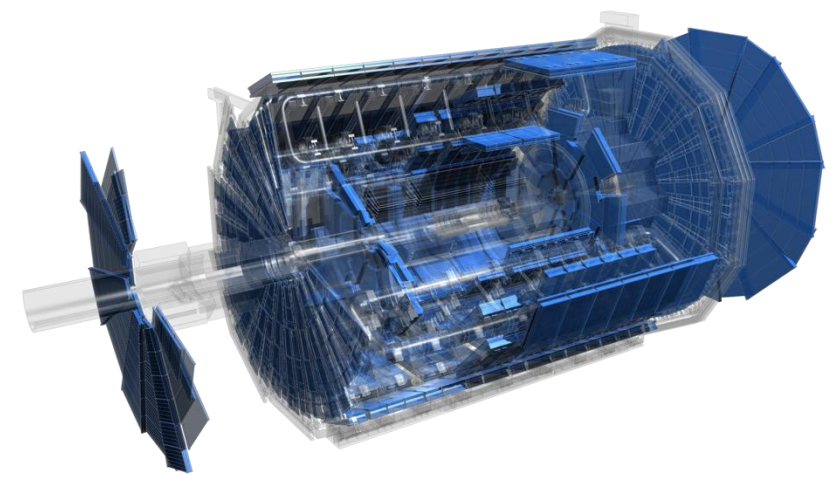
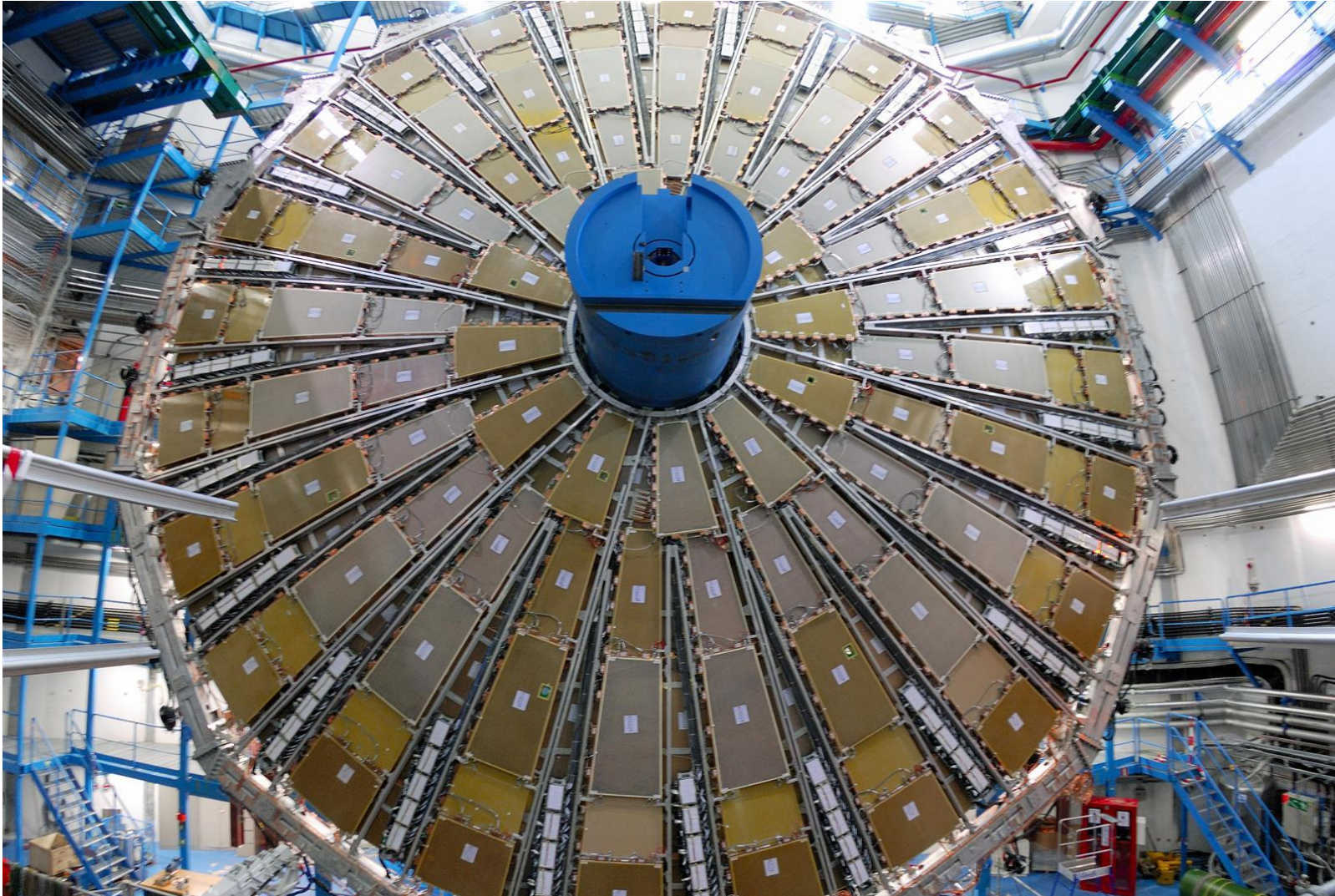
Micromegas and Small-Strip Thin-Gap Chambers (sTGCs) are two additional detector technologies specially designed for high-intensity LHC collisions. These detectors can track muons in high-density areas on either side of the experiment close to the LHC beam pipe, both quickly and with high precision.

The combined data from fast-response detectors gives a coarse measurement of a muon's momentum, allowing ATLAS to choose whether to keep or discard a collision event.

<https://atlas.cern>



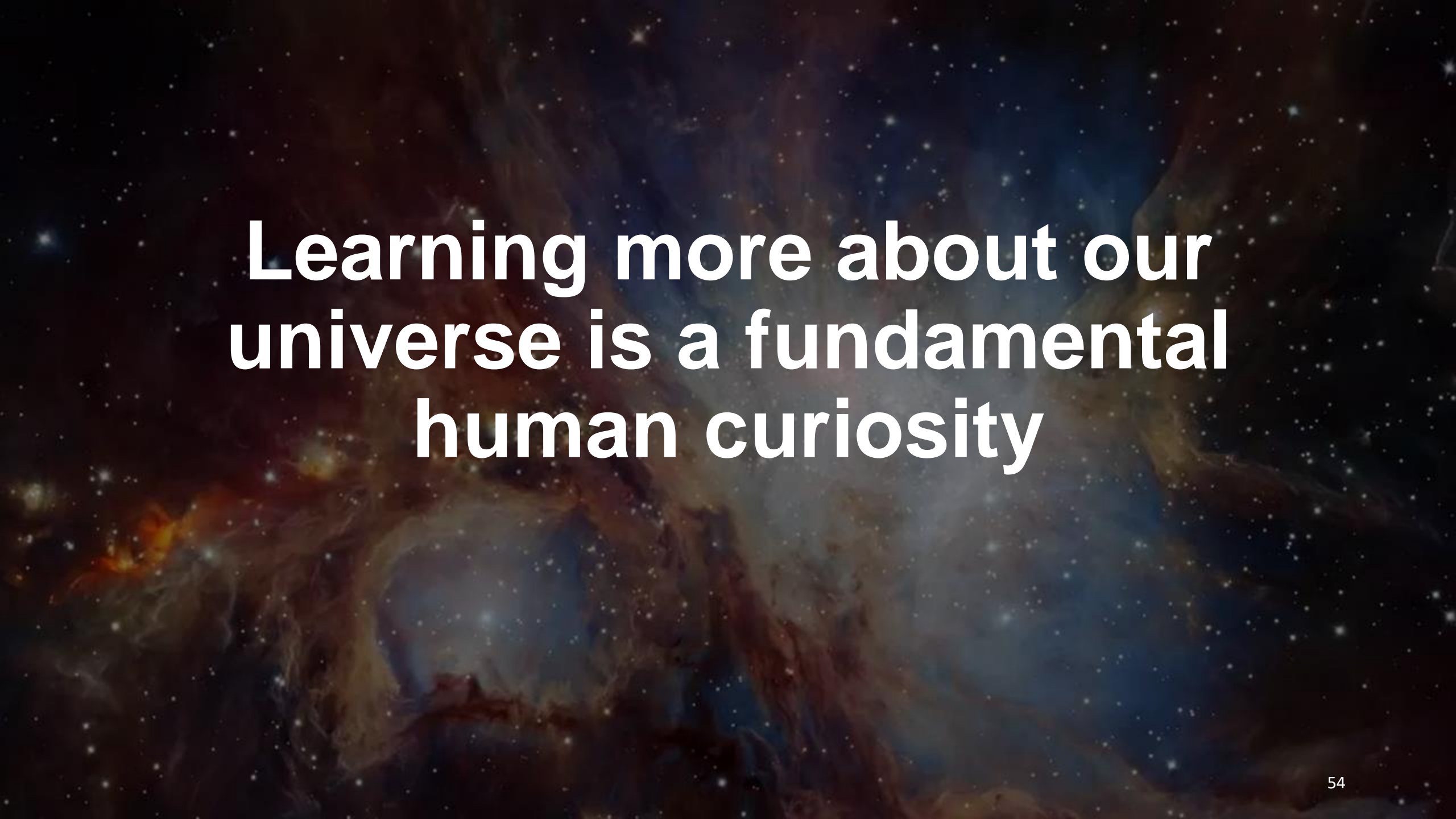
Muon Spectrometer



A visualization of particle collisions, showing a dense field of white rectangular blocks representing particles moving and colliding within a dark blue, grid-like structure. The blocks are scattered across the frame, with some appearing to converge or diverge from a central point, suggesting a high-energy collision event.

600 million collisions
every second

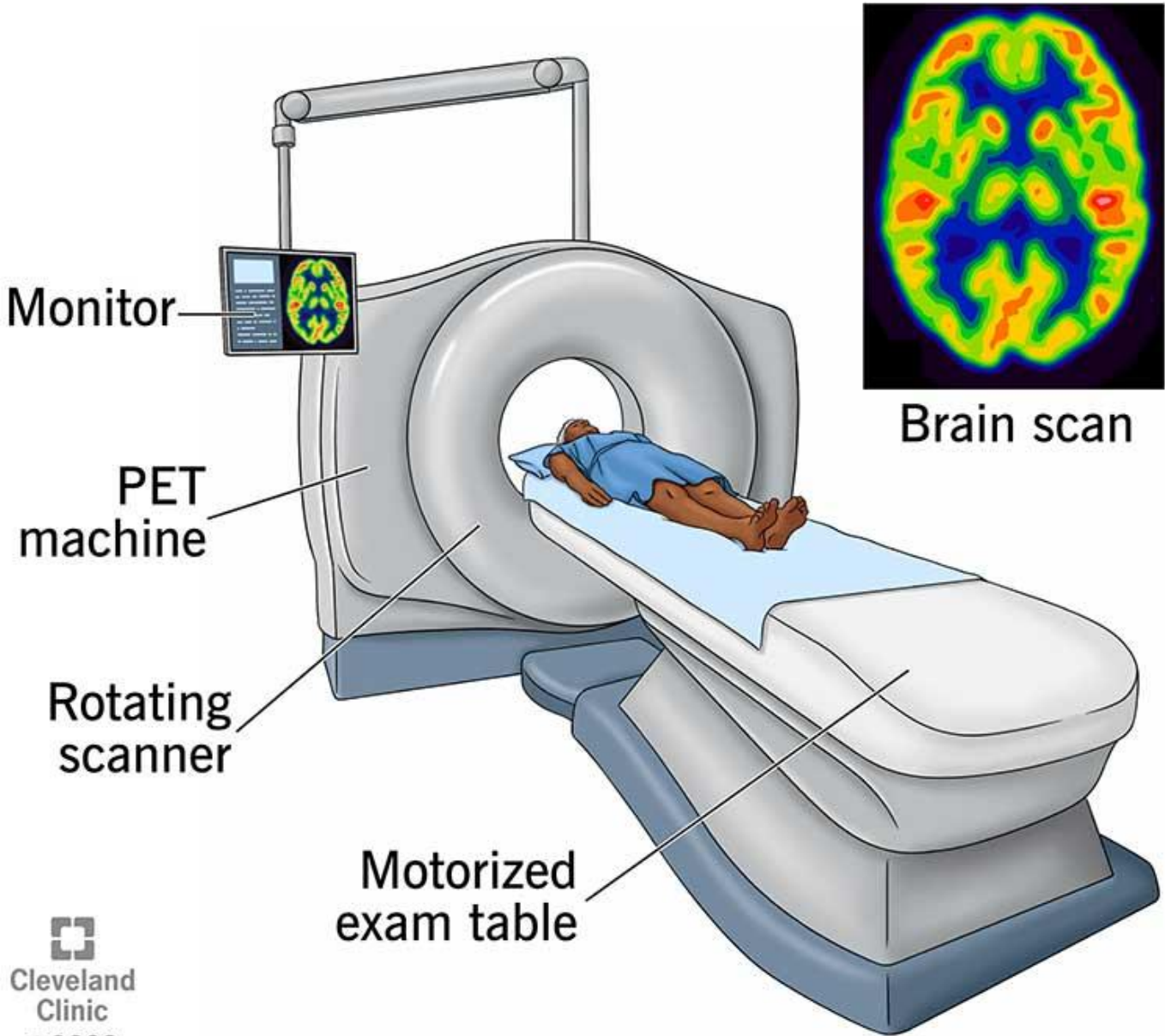
<https://videos.cern.ch/record/1541893>
(again, with energetic music :D)

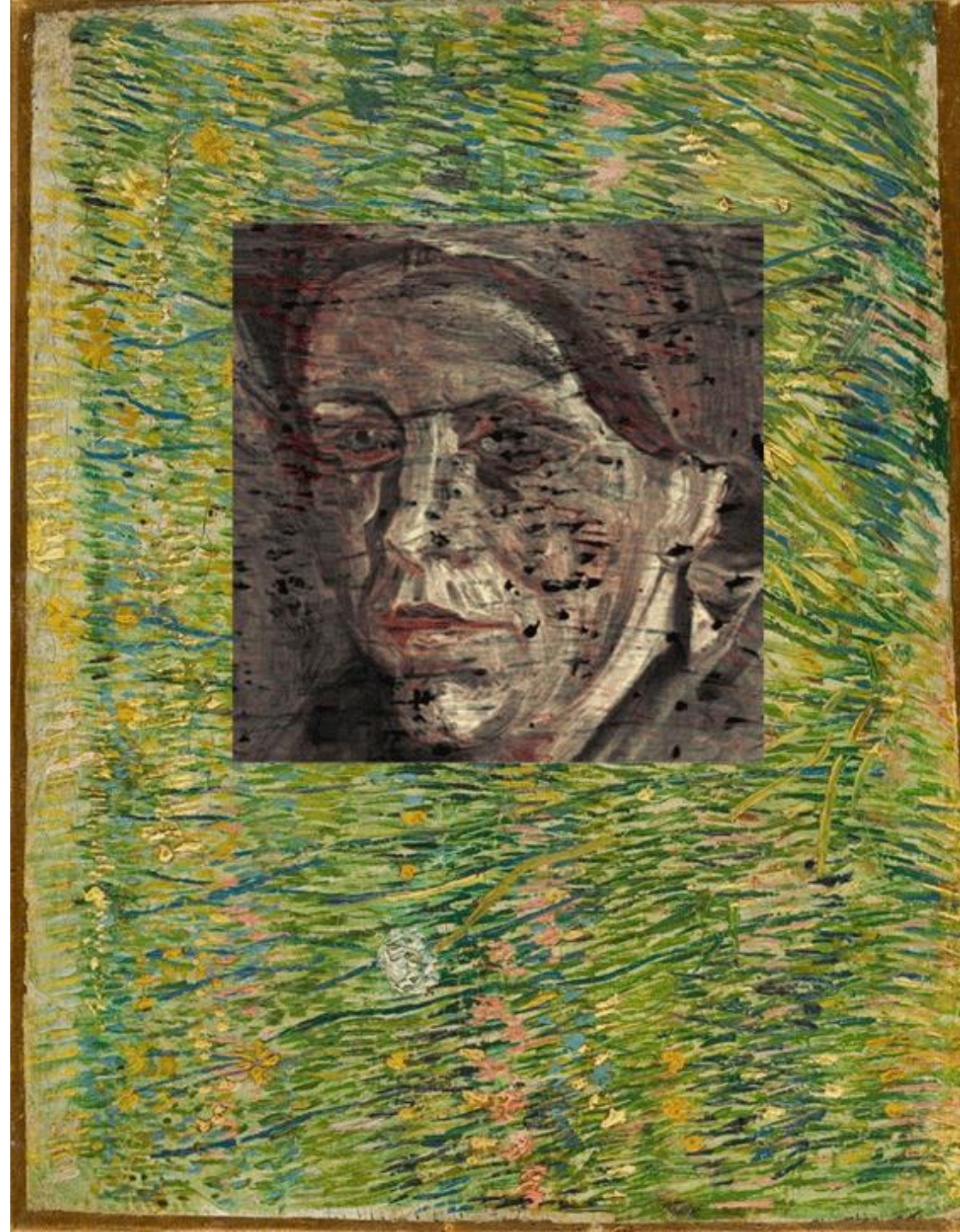


**Learning more about our
universe is a fundamental
human curiosity**

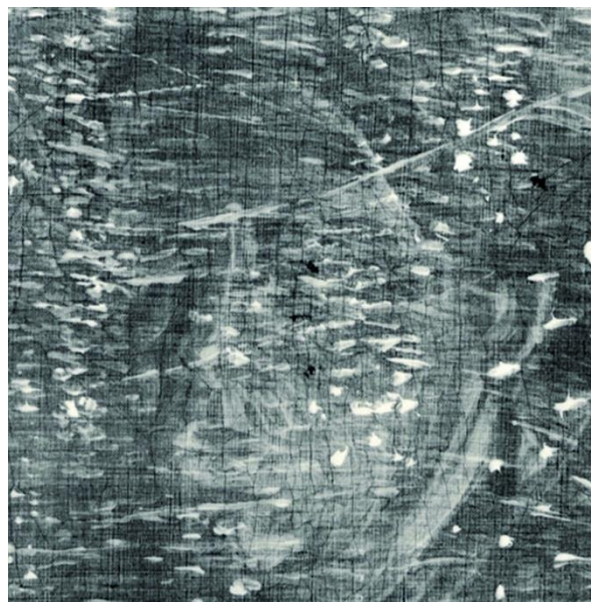
Doing difficult things gives us better technology that improves our lives and tells us interesting things right now!

PET Scan





**Synchrotron
Radiation Based
X-ray
Fluorescence
Elemental
Mapping**

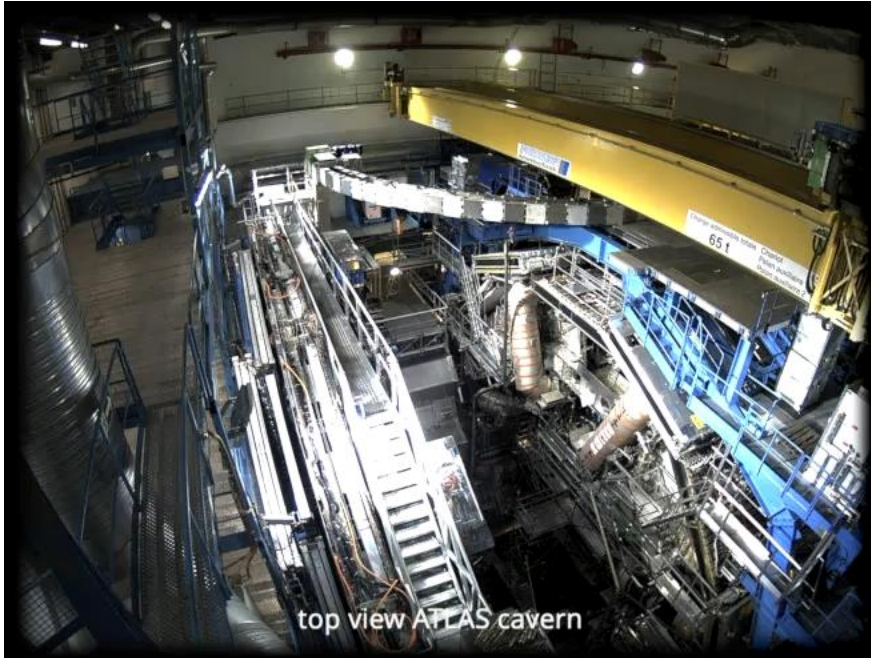


Muon tomography for pyramids



FUTURE



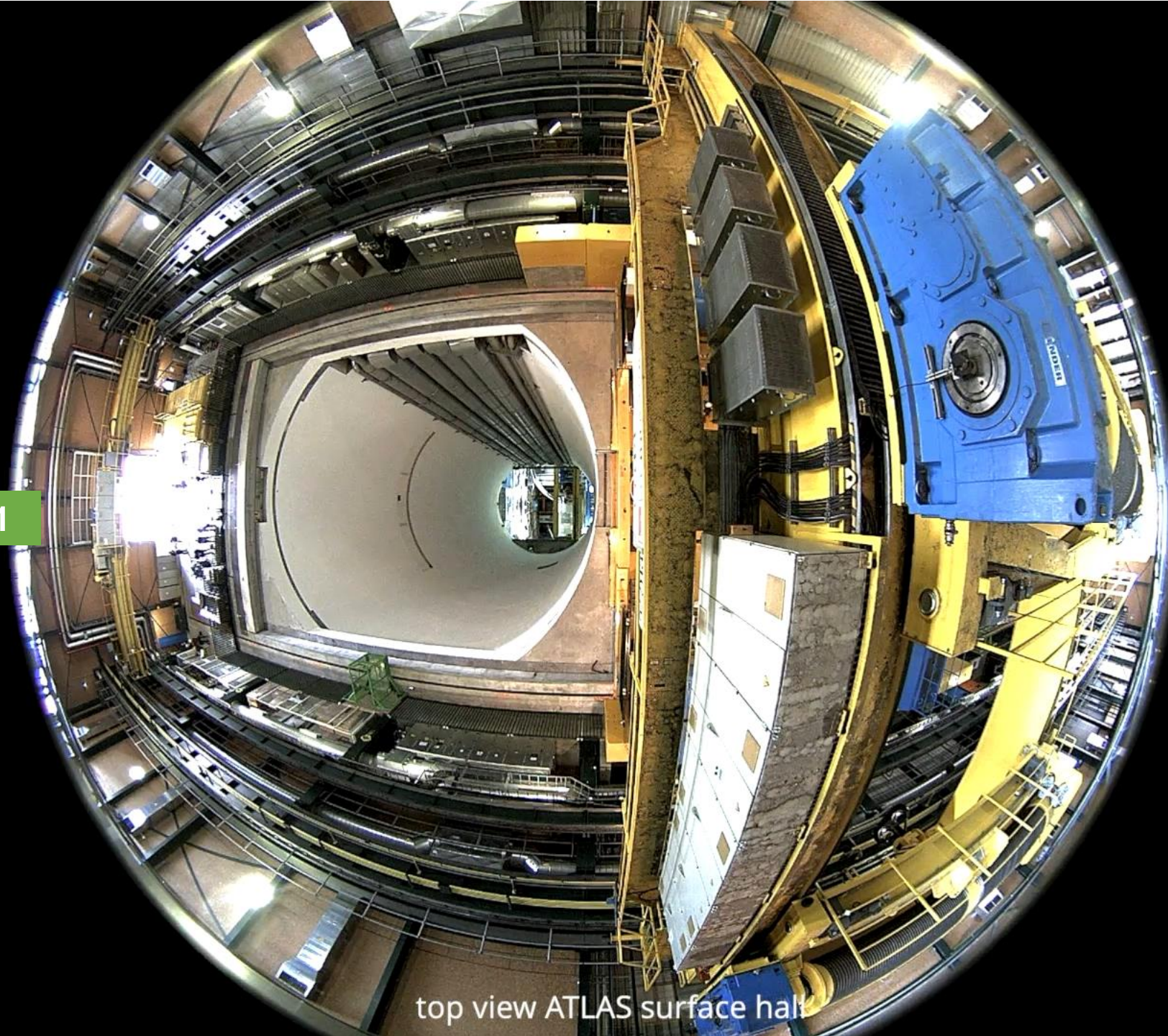


top view ATLAS cavern

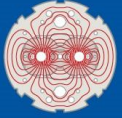
<https://videos.cern.ch/record/2776371>



level 6 ATLAS cavern

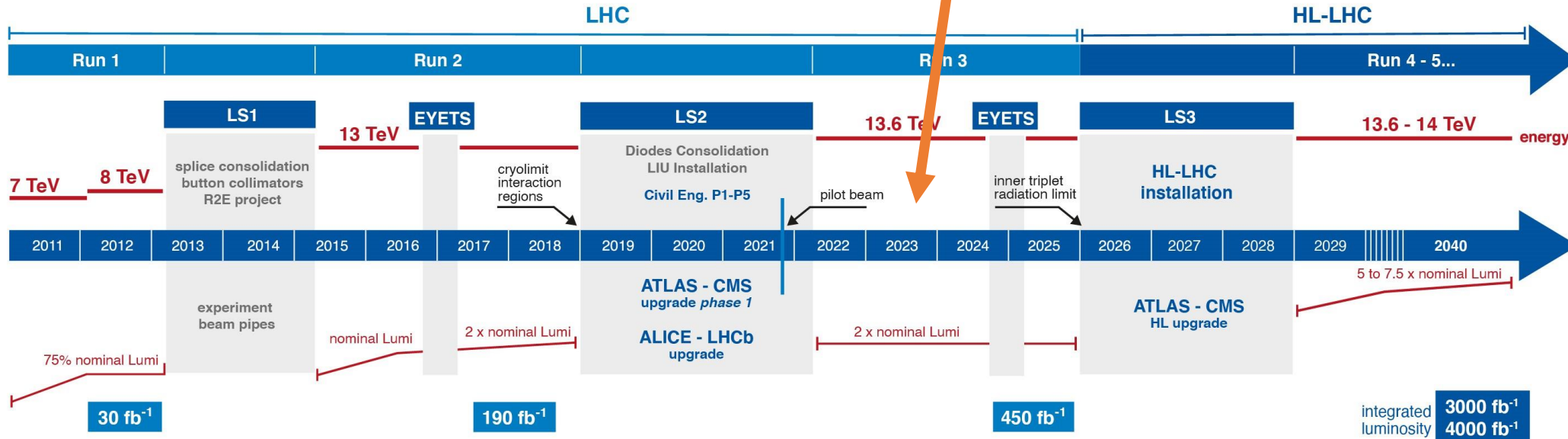


top view ATLAS surface hall



LHC / HL-LHC Plan

We are here



HL-LHC TECHNICAL EQUIPMENT:

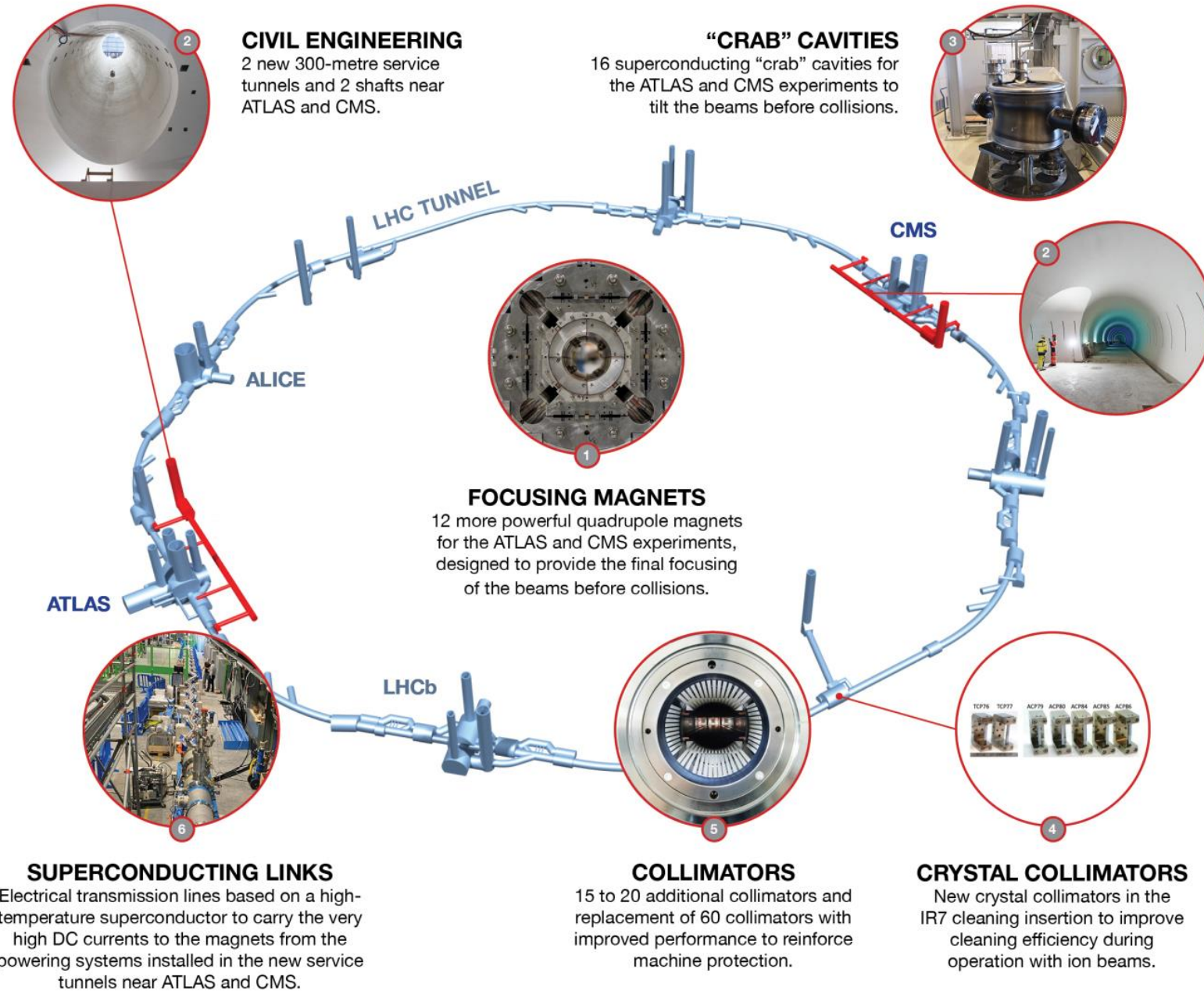


HL-LHC CIVIL ENGINEERING:



Have only taken ~ 7% of planned data so far

A new LHC Towards high luminosity



2040 and after

The future

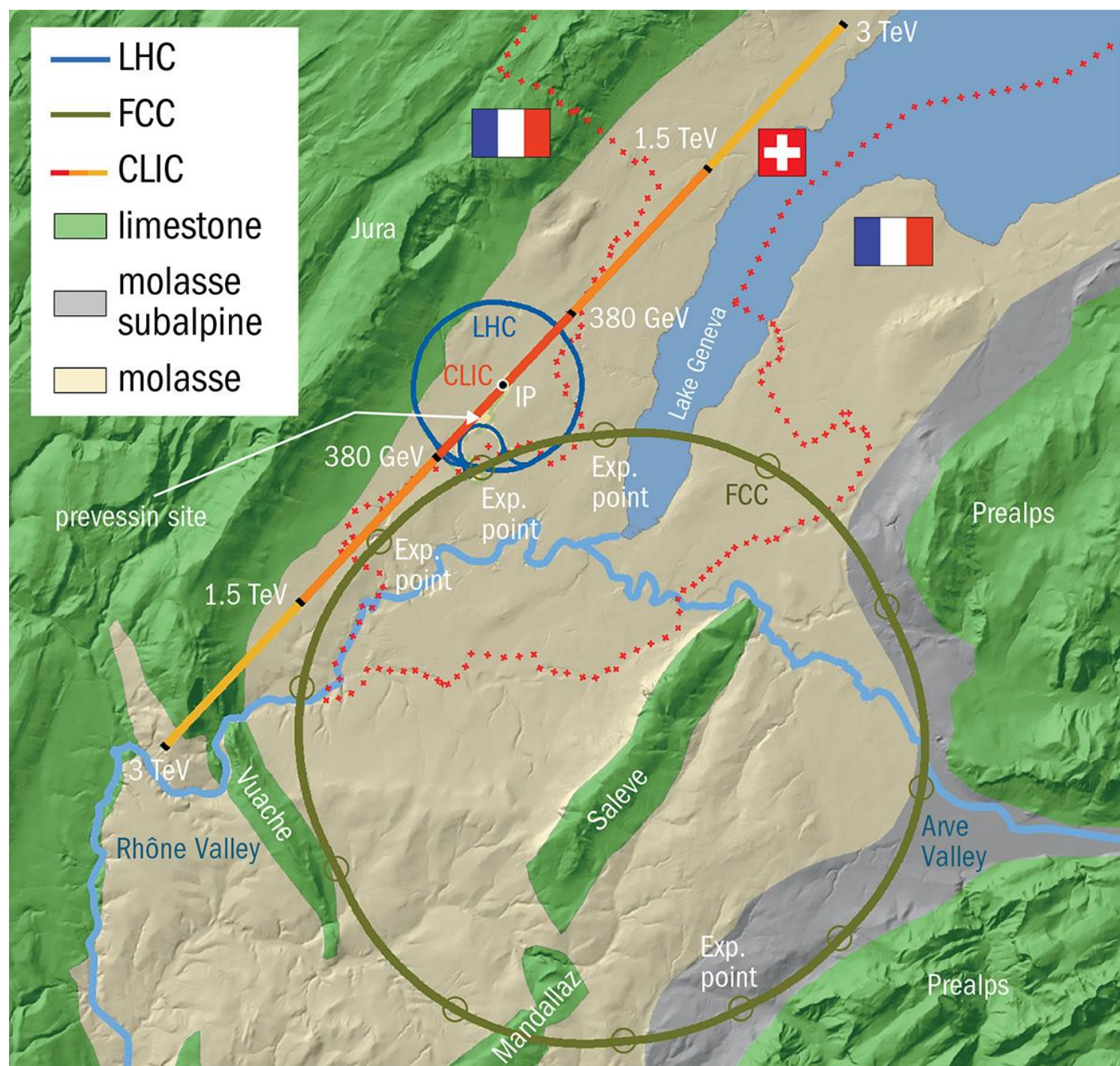
What's beyond the HL-LHC?

For the FCC we need magnets with strength of 16 T

- We don't have this yet
- Need R&D!

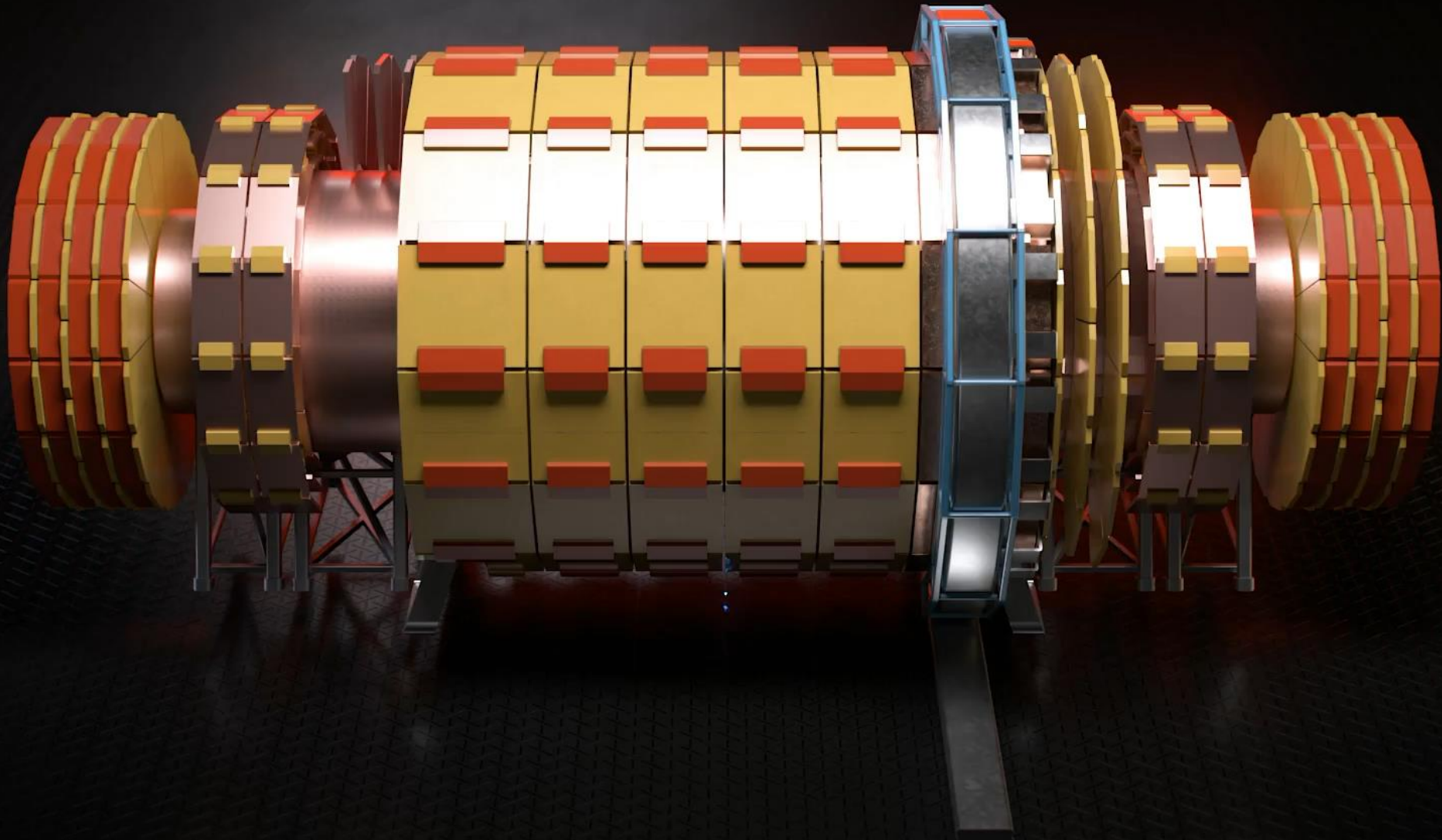
Also, muon colliders, plasma wakefield accelerators...

Linear collider?



Circular collider?

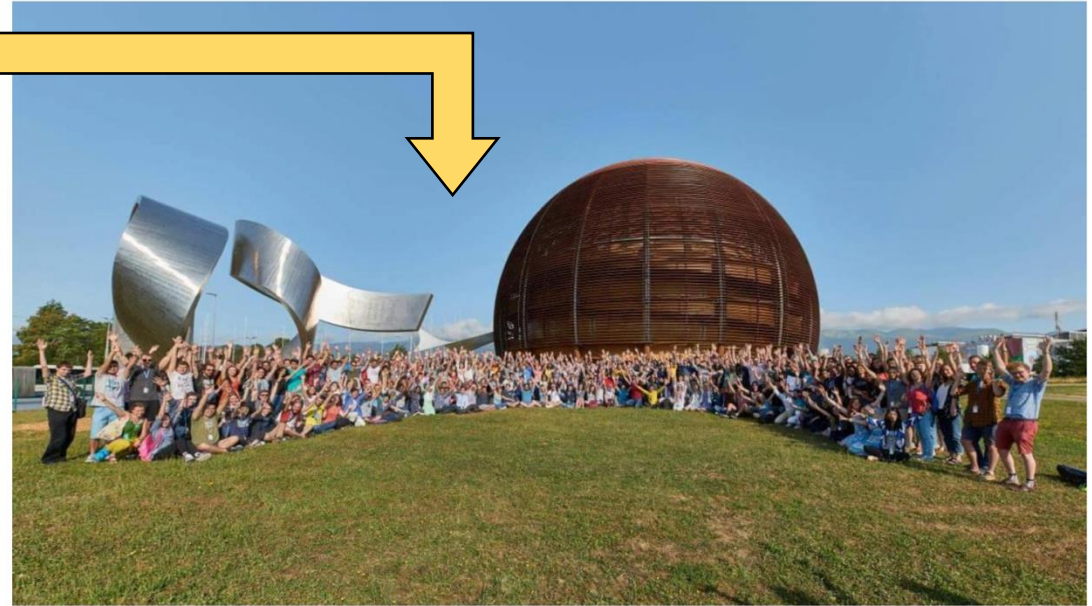
<https://videos.cern.ch/record/2299641>



Your future

There are a number of summer programmes and internships you can apply to throughout your undergraduate programme.

Apply to **EVERYTHING** you're interested in.



"I don't know if we were particularly lucky, but I really enjoyed every aspect of the summer student program: work, lectures and social life (a lot!)."

Summer programmes:

CERN Summer Student Programme
DESY Summer Student Programme
HASCO Summer School

Internships:

CERN Technical Student programme
ESA Student Internships



Thank
you!

Backup

Here's one I prepared earlier